1-1-1980

A mechanical device to study fatigue crack propagation in compact tension specimens under cyclic loading.

Timothy P. Brinker

A MECHANICAL DEVICE TO STUDY FATIGUE CRACK PROPAGATION IN COMPACT TENSION SPECIMENS UNDER CYCLIC LOADING

by

Timothy P. Brinker

A Thesis

Presented to the Graduate Committee

of Lehigh University

in Candidacy for the Degree of

Master of Science

in

Mechanical Engineering and Mechanics

Lehigh University

1980

ABSTRACT

The design of a device incorporating a mechanical loading system to study fatigue crack propagation using compact tension specimens has been completed. The machine has the capability of loading the specimen from a minimum of zero load up to a maximum of seventy-six thousand newtons. Any cyclic load range within this upper and lower bound is achievable by changing a system of static weights. Provisions for collecting fatigue crack propagation data while the specimen is subjected to various aggressive environments have been incorporated in the design. An environmental chamber which can be accommodated by the device has been proposed. A simplified device was built to test the loading scheme. Data taken using this device is compared to data taken using a servo-hydraulic test machine.

This thesis is accepted and approved in partial fulfillment of the requirements for the degree of Master of Science.

May 8, 1980
(date)

Professor in Charge

Chairman of Department

ACKNOWLEDGEMENTS

I wish to express my appreciation to my advisor Dr. Richard Roberts for his guidance and advice in the work leading to this report. I also extend a most sincere "Thanks" to Jone Svirzofsky for doing a fine job in typing. Finally, the patience and understanding of my wife, Mary Ann, during the many nights I spent at Coxe Lab, is greatly appreciated.

TABLE OF CONTENTS

1. Introduction

This report has its origin in an extensive five year federally funded program for the Federal Highway Administration of the Department of Transportation. Two of the main areas of interest within the program are (1) to study the effects of various corrosive environments on fatigue crack propagation in bridge steels, and (2) to obtain information in regard to threshold levels of fatigue crack propagation at cyclic frequencies of one hertz or less both in benign and aggressive environments.

A typical curve showing the three regions of fatigue crack growth is given in figure 1 where $\frac{da}{dN}$ is the fatigue crack growth rate per cycle and ΔK is the stress intensity factor range.

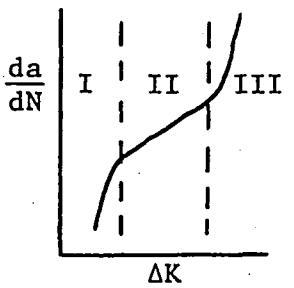

Fig. 1

The limiting value of the stress intensity factor range in region I below which a fatigue crack will not propagate, is known as the threshold value of the stress intensity factor range, ΔK_{TH}. The threshold growth rates of region I are defined by growth rates on the order of 1×10^{-7} mm/cycle.

In region II the fatigue crack propagation behavior can be modelled by the Paris equation:

$$\frac{da}{dN} = A(\Delta K)^n$$

Thus, a plot of $\log(\frac{da}{dN})$ versus $\log(\Delta K)$ in region II will yield a straight line whose slope is numerically equal to the constant n.

Some fatigue crack propagation data was collected during testing of compact tension specimens as part of the work reported here. The material tested was a 1035 grade steel with the following mean material properties:

Yield Stress	365.8 MPa
Tensile Strength	544.7 MPa
Elongation in 203.4 mm	24.1%
Area Reduction	55.3%

This material was used in the testing because it was immediately available and because it was one of the steel grades which was to be tested in the DOT project. Thus, the data collected could be used as a baseline for data to be collected in the DOT project. A proposed ASTM load shedding test procedure was used during the testing to evaluate its ability to facilitate the determination of ΔK_{TH} in a reproducible manner. The procedure was found to be acceptable and will be used in the DOT project testing.

The test is begun by precracking the specimen at a stress intensity factor range, ΔK, high enough to facilitate the initiation of a fatigue crack. Once a crack is established, the load range, ΔP, is decreased in a series of steps to decrease ΔK. This is accomplished by decreasing the load by ten percent each time the fatigue crack has extended a distance not less than the plastic zone radius determined from:

$$r = \frac{1}{2\pi}\left(\frac{K}{\sigma_{ys}}\right)^2, \quad [1]$$

where σ_{ys} is the yield strength of the material. Crack length, a, and the number of applied load cycles, N, are recorded. The crack length is determined using a traveling microscope. A typical increment of crack extension is taken as 0.5 mm. This load shedding procedure is followed until ΔK_{TH} is determined. ΔK is then allowed to increase by maintaining the load range at a constant value. a-N data is then taken with ΔK increasing. The slope of the curve plotted from the a-N data is the crack growth rate, $\frac{da}{dN}$. Thus, from the a-N data a curve representing the crack growth rate versus the stress intensity factor range can be constructed.

When testing at low values of the stress intensity factor range a relatively large number of load cycles must be

[1]Stanley T. Rolfe and John M. Barsom, Fracture and Fatigue Control in Structures (Englewood Cliffs, New Jersey: Prentice-Hall, 1977), p. 60.

applied to the specimen in order to determine ΔK_{TH}. The average number of load cycles required to smoothly decrease ΔK down to ΔK_{TH} and then allow ΔK to smoothly increase, was approximately forty-seven million cycles. At a loading frequency of fifty hertz, the tests required two hundred sixty five hours to complete. Figure 2 shows a plot of the data taken during these tests. The threshold stress intensity factor range for this 1035 steel is seen to be approximately 3.3 $MPa\sqrt{m}$ at a load ratio of 0.8.

The data for the DOT project is to be collected while operating at a frequency of one cycle per second, as this loading frequency has been determined to be representative of loading rates seen by bridges. Since the average number of cycles of loading during the threshold test was forty-seven million, the time required to complete the test at a frequency of one hertz is 13250 hours, or about 1.5 years. Clearly, a device which could be built economically to reliably do the testing was desirable. Because the effects of aggressive environments on fatigue crack propagation were to be studied, the machine must have the capability of accommodating some sort of environmental chamber. With a chamber surrounding the test specimen, optical measurement of the crack length would be difficult, if not impossible. A compliance technique was chosen as being a viable method of determining the crack

Figure 2

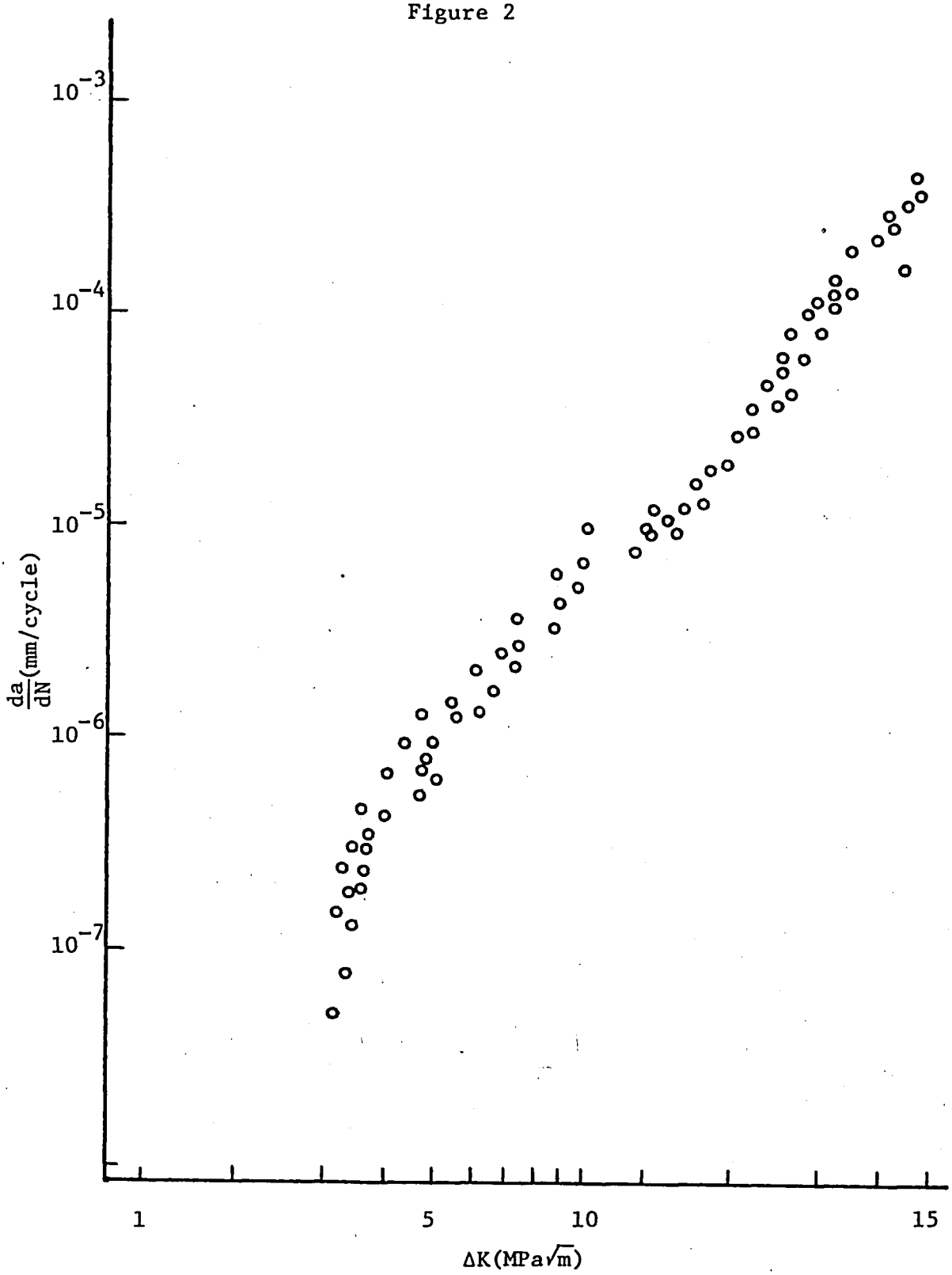

length under these conditions. The crack opening displacement would be measured using a linearly varying displacement transducer, LVDT.

When testing with the more conventional servo-hydraulic machines, a current off-current on situation, or any event which might cause a deviation in the load waveform, could result in an overload to the specimen. An overload is a single or multiple application of a load larger in magnitude than the maximum load intended to be applied to the test specimen, and has the effect of delaying the growth of the fatigue crack by locally yielding the material at the crack tip. Since it is extremely inconvenient to obtain a history of the loading because of the large number of loading cycles, there is no way of assuring that every load cycle is exactly the same as the cycle before. Therefore if an overload would occur, an accurate evaluation of the magnitude of the overload and the resulting delay would be impossible. The relative ease with which an anti-overload scheme could be incorporated in the design, as well as economy, reliability and corrosion fatigue testing capabilities, made a mechanical device an attractive and practical alternative to the servo-hydraulic test devices. The economy of the mechanical device is realized when the 0.2 H.P. required to power the mechanical device is compared to the 20 H.P. required for a typical hydraulic unit.

With the goal of developing a machine with the above features in mind, this report proceeds.

2. Initial Design

A mechanical loading system, as compared to a servo-hydraulic system, was chosen for its simplicity as well as for ease at which an anti-overload safeguard could be built in. The loading system consists of a set of weights attached to the specimen as in figure 3.

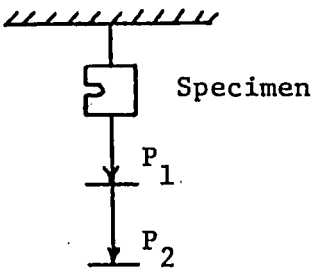

Fig. 3

That portion of the load due to P_2 is removed by means of a cam device while load P_1 is maintained. Load P_2 is then reapplied. In this manner a loading cycle is established. The maximum load which can be applied to the specimen is the sum of P_1 plus P_2. The loading cycle is shown in figure 4.

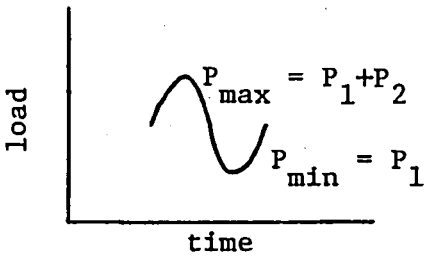

Fig. 4

The shock imparted to the specimen due to sudden application and removal of load P_2 was reduced by using a system of precision compression springs. A cam device drives

a spring-plate system to smoothly remove load P_2. On the downward part of the cam cycle, load P_2 is smoothly reapplied (figure 5).

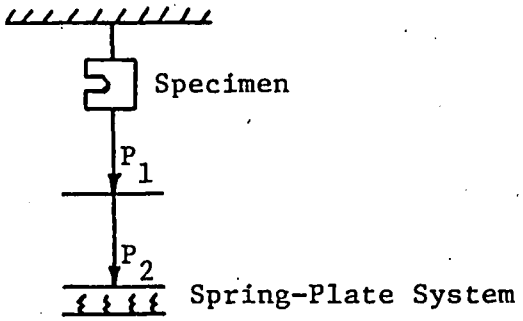

Fig. 5

The maximum load P_{max} is then applied when clearance is observed between the compression springs and load P_2. Load P_2 is removed when clearance is observed between a washer at the end of the rod connecting load P_2 to load P_1, and P_2 (figure 6)

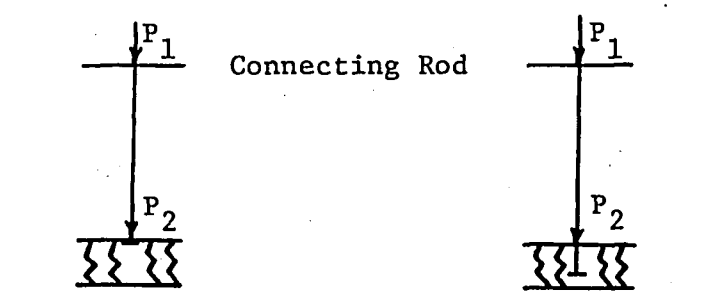

Fig. 6

A photograph of a device incorporating this loading scheme is shown in figure 7. This device was built at Lehigh University and was used to test the loading scheme described above.

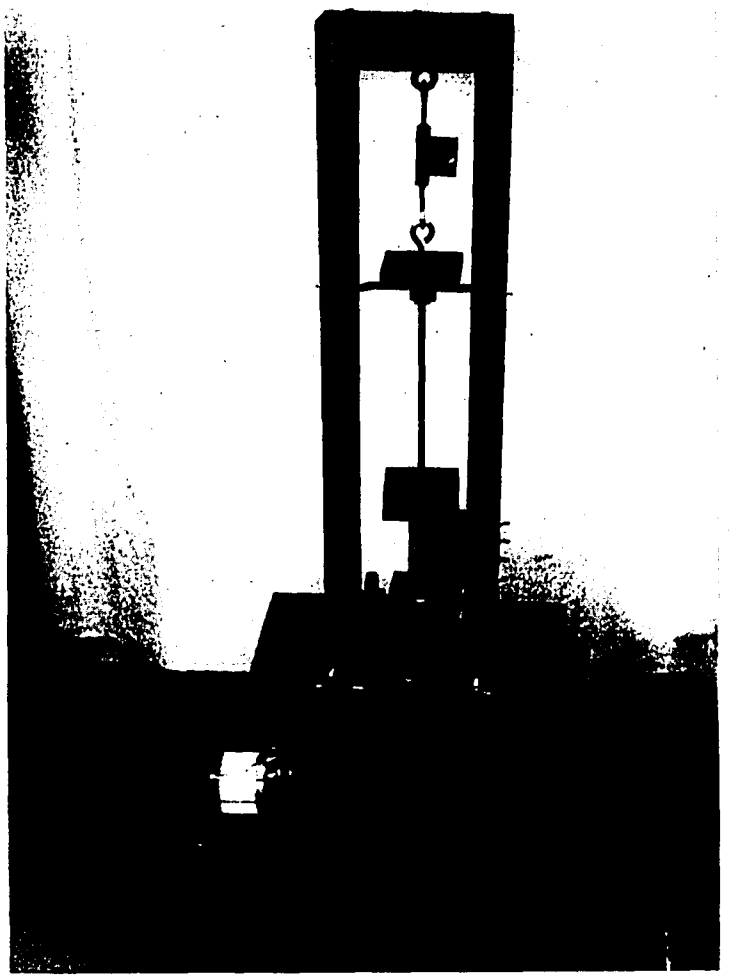

Figure 7.

3. Test of Loading Scheme

If the simple mechanical loading system was to be used to generate data for the five-year study, it would have to be shown that the system could reliably reproduce results of data taken using the more conventional servo-hydraulic test machines. Consequently, two tests were run simultaneously, one using the servo-hydraulic device and the other using the mechanical device. The specimens were of the compact tension configuration shown in figure 8.

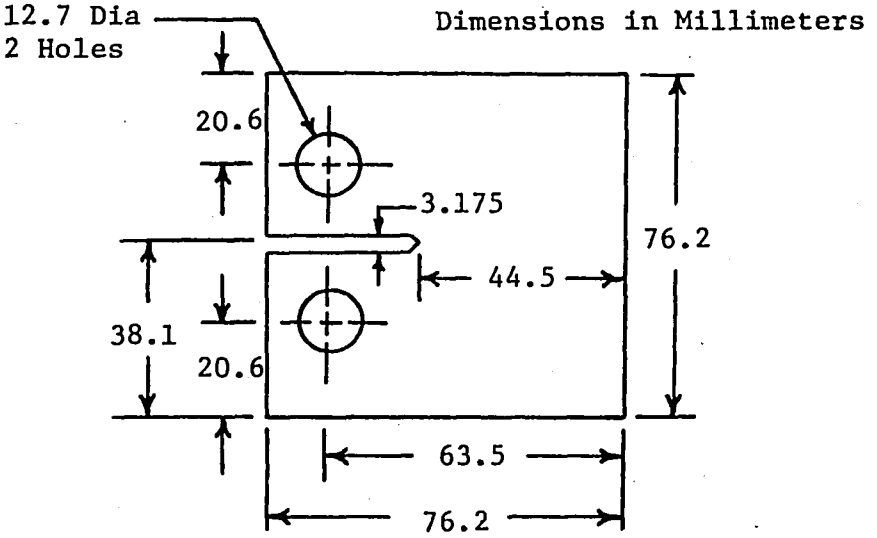

Fig. 8

After machining, the specimens were polished using 600 grit carborundum paper. Polishing strokes were perpendicular to the machined notch.

The tests were to be run at a frequency of 1 cycle/sec. To facilitate the initiation of a fatigue crack in a reasonable

amount of time, both specimens were precracked on a servo-hydraulic test machine at forty hertz. Because of limitations in the amount of space available, 1200 Newtons was about the maximum load the mechanical device could accommodate. From the results of previous tests (figure 2) it was known that a stress intensity factor range of $\Delta K = 14 MPa\sqrt{m}$ would yield growth rates of approximately 10^{-5} mm/cycle. Stress intensity range, load, and crack length are related by the following equation:

$$\Delta K = \frac{\Delta P}{b\sqrt{w}} f(\frac{a}{w}) \qquad (1)$$

where

$$f(\frac{a}{w}) = 0.2960(\frac{a}{w})+1.855(\frac{a}{w})^2+6.557(\frac{a}{w})^3-10.17(\frac{a}{w})^4+6.389(\frac{a}{w})^5, \qquad (2)$$

and b, a, and w are shown in figure 9.

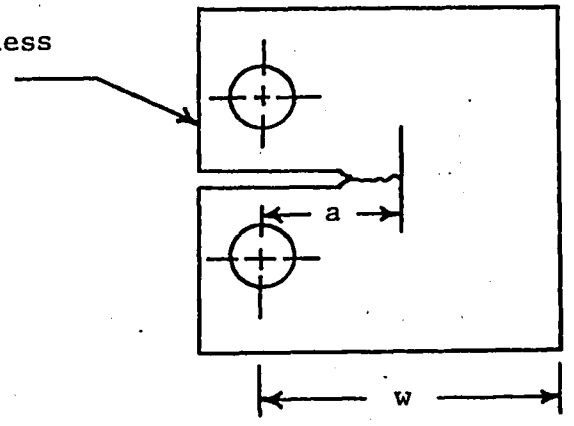

Fig. 9

[2]Rolfe and Barsom, p. 42.

The load ratio, $R = \frac{P_{min}}{P_{max}}$ was to be R=0.1. ΔP and R can be shown to be related as follows:

$$\Delta P = P_{max} - P_{min}$$

Dividing through by P_{max},

$$\frac{\Delta P}{P_{max}} = 1 - \frac{P_{min}}{P_{max}}$$

But,

$$\frac{P_{min}}{P_{max}} = R$$

Therefore,

$$\Delta P = P_{max}(1-R) \qquad (3)$$

Substituting the results of equation 3 into equation 1 yields:

$$\Delta K = \frac{P_{max}(1-R)}{b\sqrt{w}} f(\frac{a}{w})$$

$$f(\frac{a}{w}) = \frac{b\sqrt{w}}{P_{max}(1-R)} \Delta K \qquad (4)$$

All quantities on the right side of equation 4 are known and therefore the crack length necessary to produce a stress intensity range $\Delta K=14MPa\sqrt{m}$ with a maximum load of 1200 Newtons may be determined from equation 2. Carrying out the calculation yields, a=36.83 millimeters. Therefore, when the crack length reached 36.83 millimeters the loading frequency

was reduced to one cycle per second. At this point one specimen was tested on the mechanical system while the other was simultaneously tested on a servo-hydraulic test device. Crack length and number of load applications were recorded and a plot of this data is given in figure 10. For both tests, the crack length was measured using a traveling microscope. It is interesting to note that the specimen which was being tested on the servo-hydraulic device was for unknown reasons overloaded. The overload occurred sometime after the crack length of 39.6 millimeters was determined, as can be seen in figure 10. As a result of the overload a large plastic zone was established at the crack tip. This caused the fatigue crack to stop propagating. Consequently the testing of this specimen had to be terminated. Note that an overload of this type can not occur on the mechanical system. If for some reason there is a power surge or the power is shut off, the maximum load which can be transmitted to the specimen is the sum of P_1 and P_2 shown in figure 5.

A plot of $\frac{da}{dN}$ versus ΔK in figure 11 shows that comparable data was being taken from both machines up until the application of the overload.

Figure 10

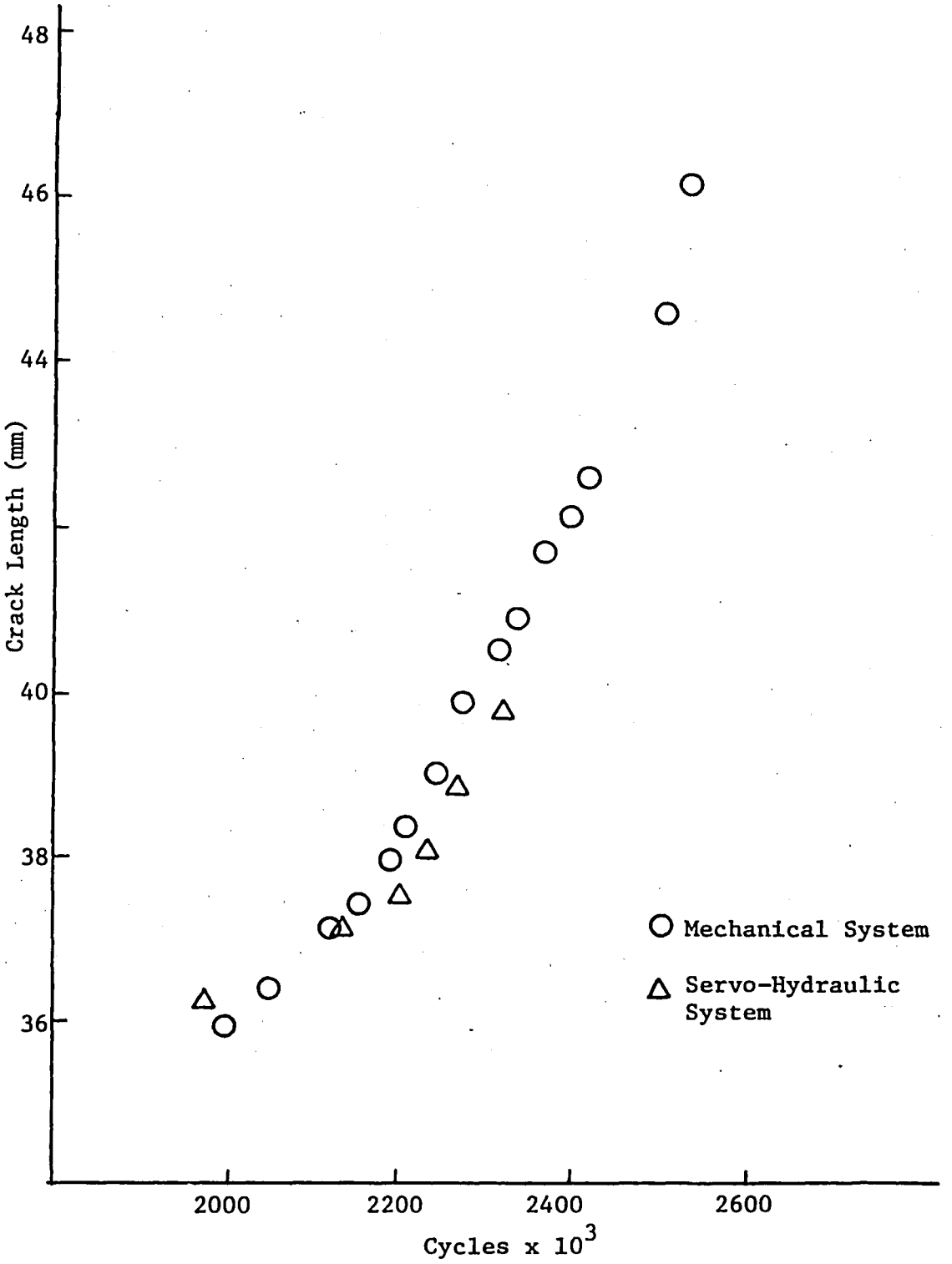
48
46
44
40
38
36
Crack Length (mm)
2000
2200
2400
2600
Cycles x 10^3
Mechanical System
Servo-Hydraulic System

Figure 11

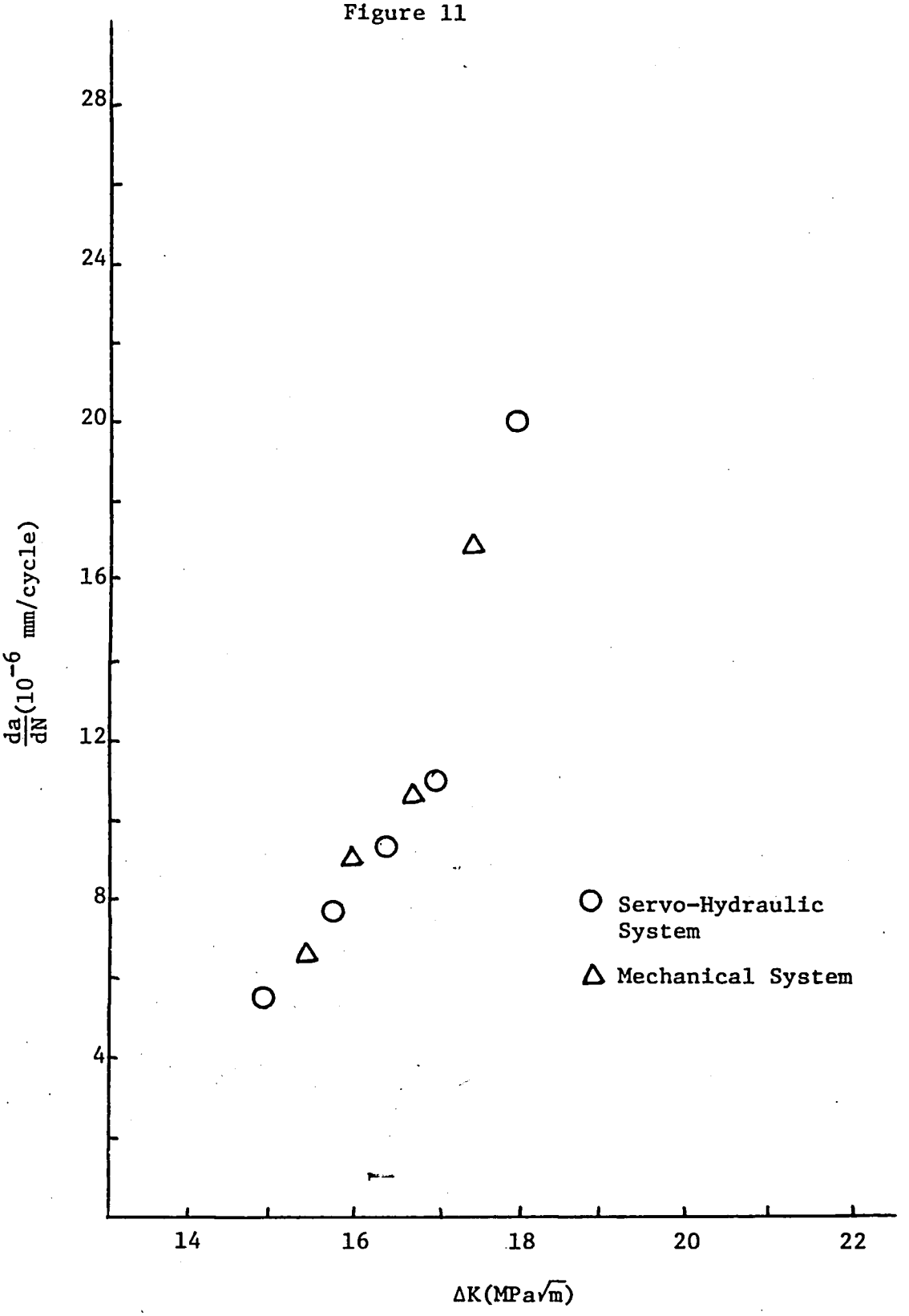
28
24
20
16
12
8
4
$\frac{da}{dN}(10^{-6}$ mm/cycle)
14
16
18
20
22
ΔK(MPa√m)
Servo-Hydraulic System
Mechanical System

4. Final Design

The final design was to have the capability of testing compact tension specimens of up to 25.4 mm in thickness. To have this capacity, loads in excess of 71000 Newtons would have to be applied to the specimen. A lever system was chosen as a viable means of decreasing the amount of weight necessary to achieve the desired loading. It can be seen in figure 12 that the lever has the effect of magnifying the load ten times.

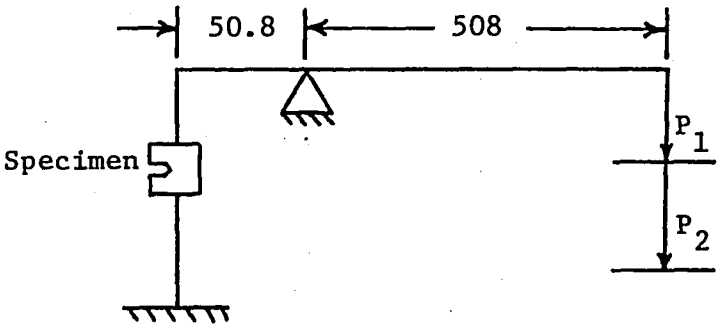

Fig. 12

A device incorporating this idea is shown in figure 13. The device consists largely of a rigid frame composed of I-beams, wide flange shapes, steel tubing and steel angle. These components were chosen for their inherent strength and availability. The lever is composed of two parallel 25.4 mm thick bars separated by a steel spacer which provides the necessary clearance for other components.

The cam which drives the spring-plate system to provide the desired fatigue loading of the specimen is shown in figure

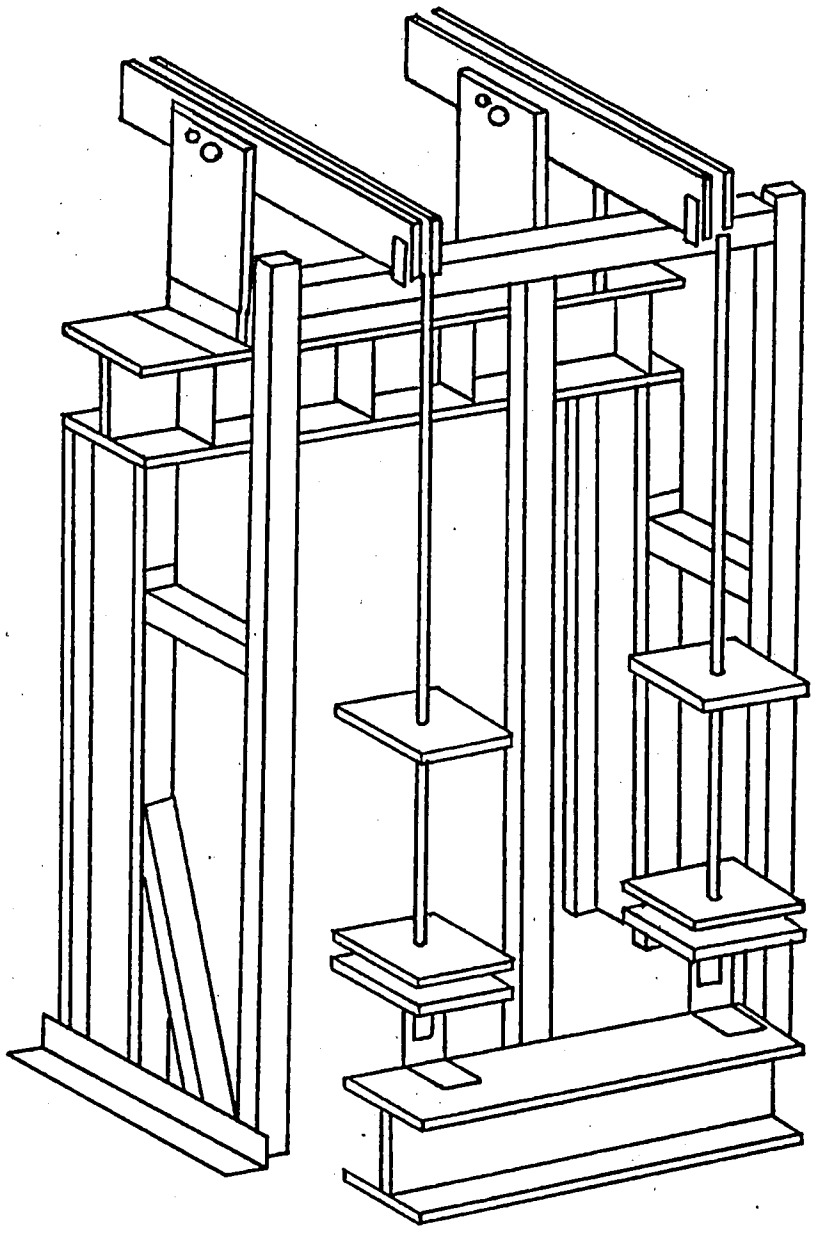

Figure 13.

14. Note that this entire assembly is to be located on the 152 mm wide flange (figure 13), but is not shown in figure 13 for ease in drawing. The necessary straight line motion of the spring-plate is guaranteed through the use of a linear pillow block bearing (figure 14).

A one hundred RPM gearhead motor drives the cam shaft at 60 RPM by using a 76.2 mm. diameter pulley on the motor and a 127 mm. diameter pulley on the cam shaft. The number of loading cycles is determined by multiplying the elapsed time by the speed of the cam shaft. In this case, multiplying the elapsed time in minutes by sixty will yield the number of cycles of loading applied to the specimen.

As described above, the lever consists of two 25.4 mm. thick bars. The pivot point of the lever is a roller bearing which is pressed into the lever support. The static weight is attached to the lever 50.8 centimeters from the pivot. The specimen is attached to the lever on the opposite side of the pivot and 5.08 centimeters from it. Mounting of the specimen to the lever is done as in figure B2, appendix B. This configuration allows an environmental chamber to be placed around the specimen and grips. A possible chamber could be a two piece construction fabricated out of clear 6 mm. thick plexiglass bonded together with a silicon based adhesive.

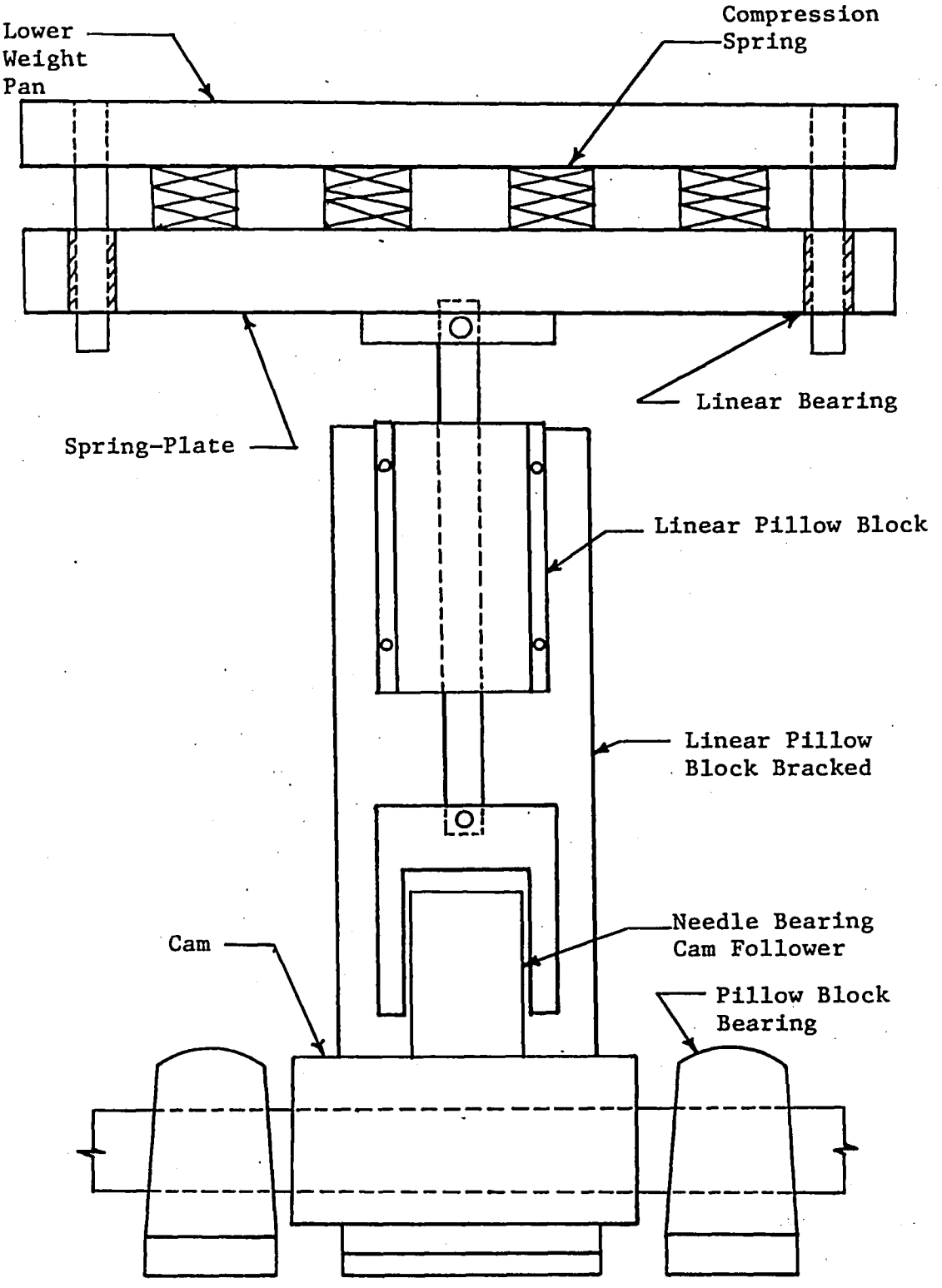

Figure 14. Loading System, Assembly

The specimen and grips may be removed from the mounting assembly by removing the two 19 mm. pins which hold them in position. With the specimen and grips removed the chamber can easily be installed. Piping to and from the chamber can be added as is needed. The crack length will be determined using a compliance technique by measuring crack opening displacement using a LVDT and therefore the chamber must be large enough to accommodate the transducer.

5. Conclusions

Mechanically the spring-plate loading system functioned reliably. On the initial design some rocking of the weights was evident while the machine was in operation. The addition of a nylon bushing to guide the rod connecting the two weight pans decreased the rocking motion to an acceptable level.

Although only a limited amount of data is available to compare the device to the servo-hydraulic test machine, the data which was taken indicates that comparable growth rates can be achieved on both test machines.

Compared to the conventional test devices, the mechanical device is relatively inexpensive. Coupled with its simplicity is an anti-overload feature. Therefore, based on the ease with which the device can be constructed, reliability and cost, it is concluded that the device should be considered for use in the DOT project.

REFERENCES

1. Rolfe, Stanley T. and Barsom, John M., Fracture and Fatigue Control in Structures. Englewood Cliffs, New Jersey: Prentice-Hall, 1977

2. Shigley, Joseph E., Mechanical Engineering Design. New York: McGraw-Hill, 1977.

APPENDIX A

CALCULATIONS

The design loads of the device will be based on the loads which would be necessary to test a 25.4 millimeter thick compact tension specimen with w=5.0 (figure 8) at a load ratio of R=0.8. This is a conservative approach since the device will be primarily used to test the standard ASTM 1-T compact tension specimen and therefore considerably lower loads will be required. All components of the device which are part of the load path will be included in the analysis. The load path passes through the spring-plate, through the connecting rods, along the lever and into the specimen mounting assembly. A minimum factor of safety of four will be used in all calculations except for bearings where size is a limiting factor.

Bearing Selection

1. Cam Follower

Under the above criterion, ΔP_{max}=18680N. Therefore the maximum load that the cam follower will be subject to is 1868N. The following factors are taken from Torrington Catalog #478:

Speed Factor at 60 RPM = 1.2

Life Factor for 35000 Hours = 3.6

Factor of Safety = 3.0

Then,

$$(1.2)(3.6)(3.0)(1868) = 24209.28$$

Choose bearing YCR ∿32

2. Pillow Block Bearing

Load Capacity at 60 RPM = 8896 N

Life Factor for 35000 Hours = 2.6

Capacity for 35000 Hours = $\frac{8896}{2.6}$ = 3421.5 N

The maximum operating load of the cam is 1868 N, therefore the maximum load to which the pillow block bearings are subjected is 934 N. The 25.4 mm. RAK Fafnir pillow block bearing is adequate for this application.

$$\text{Factor of Safety} = \frac{3421}{934} = 3.66$$

3. Roller Bearing

A roller bearing is used at the pivot point of the lever. The maximum load at each bearing is 27522 N.

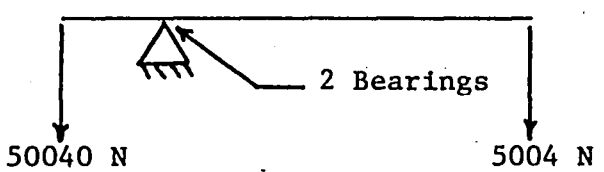

Speed Factor at 60 RPM = 1.2

Life Factor for 35000 Hours = 3.6

Then,

$$(1.2)(3.6)(27522) = 118895$$

Choose bearing HJ-526832 with an inner race. The use of an inner race eliminates the need of using a hardened shaft as well as reducing the diameter of the shaft required.

Lever

The lever is a 25.4 mm. x 102 mm. x 813 mm. cold rolled steel bar with a yield strength of 379 MPa. Therefore the allowable stresses are:

$$\sigma_{ALL} = \frac{379}{4} = 94.75 \text{ MPa}$$

$$\tau_{ALL} = 47.375 \text{ MPa}$$

1. Shearing of the bearing shaft through the lever material

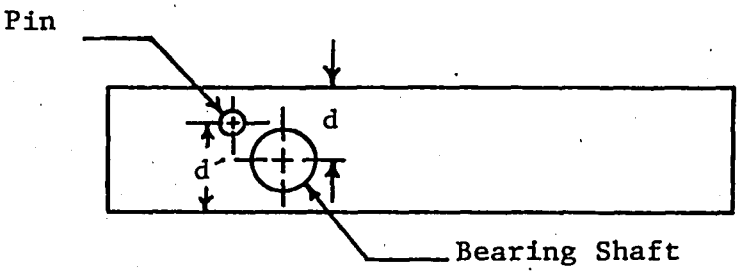

$$d_{min} = \frac{F_{max}}{2t\tau} = \frac{102304/2}{2(25.4)(47.375)} = 21.26 \text{ mm}$$

2. Shear of pin through the lever material

$$d'_{min} = \frac{93097/2}{2(25.4)(47.375)} = 19.34 \text{ mm}$$

3. Bending stress in ligament above roller bearing

$$\sigma = \frac{MC}{I} = \frac{(508)(9307.7)(51)12}{2(25.4)(102)^3} = 54.7 \text{ MPa}$$

This stress is less than the allowable stress.

Grips

The grip material is cold rolled 1018 steel. Using a factor of safety of 2, the allowable shear stress is 94.75 MPa.

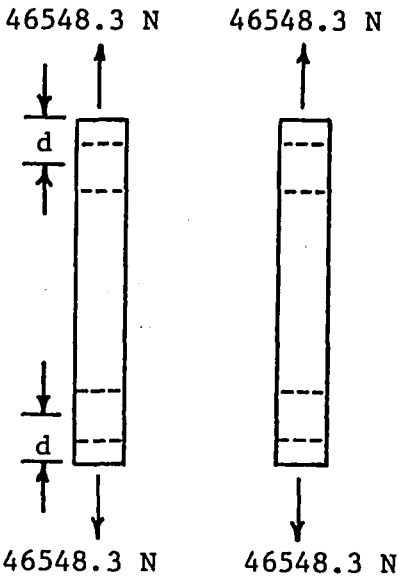

$$d_{min} = \frac{46548.3}{2(16)(94.75)} = 15.35 \text{ mm.}$$

Choose d = 16.5 mm. The factor of safety then becomes F.S. = 2.16

Deflection of Upper 152 mm Wide Flange

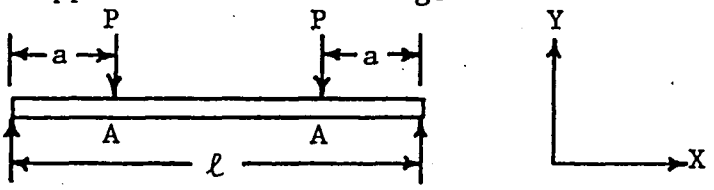

$$y_A = \frac{Pa}{6EI}(4a^2 - 3al)$$

where, a = 343.5 mm and l = 1372 mm.

Therefore,

$$y_A = \frac{(9296.3)(343.5)}{(6)(2.0682\text{x}10^5)(2231)} [4(34.35)^2-3(34.35)(1372)]$$

$$y_A = -.109 \text{ mm.}$$

The maximum deflection is,

$$y_{max} = \frac{Pa}{24EI} (4a^2-31^2)$$

$$y_{max} = \frac{(9296.3)(343.5)}{(24)(2.0682\text{x}10^5)(2231)} [4(34.35)^2-3(1372)^2]$$

$$y_{max} = -.149 \text{ mm}$$

Buckling of 152 mm I-beam

The critical load is:

$$P_{CR} = \frac{\pi^2 EI}{1^2} = \frac{\pi^2(2.0682\text{x}10^5)(41.623)}{(137.2)^2}$$

$$P_{CR} = 1.174\text{x}10^7 \text{N}$$

This load is well below the actual operating loads of the device.

Angle Mounting Lever to 152 mm Wide Flange

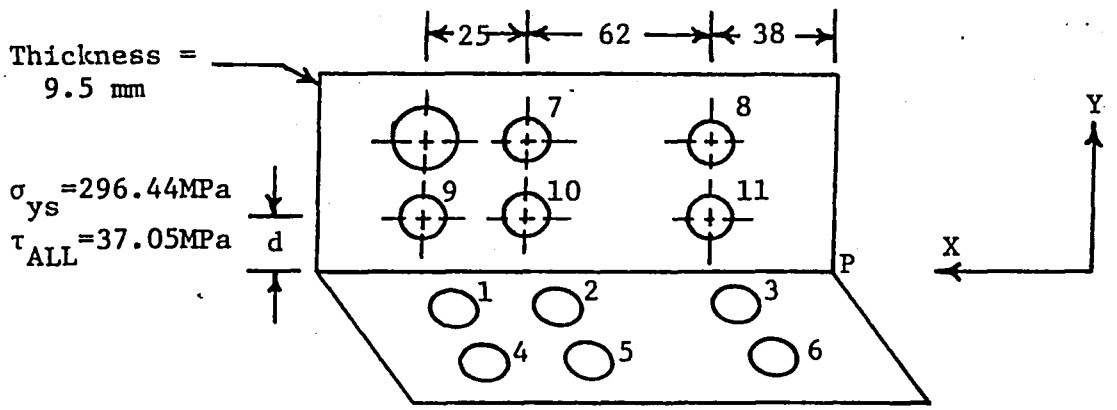

1. Bolts #1 through #6 will be in tension due to the eccentric load applied through the lever. The centroid of this bolt group is located 87.66 mm. from point P, in the X-direction.

$$\bar{x} = \frac{2(38)A+2(100)A+2(125)A}{6A}$$

$$\bar{x} = 87.66 \text{ mm.}$$

Here A is the cross-sectional area of the bolt.

Then summing forces about point P we can calculate the effective force Q acting at the centroid.

$$Q = \frac{432(9309.7)}{87.66} = 45879.4 \text{ N.}$$

Then using 16 mm. bolts, for twelve bolts,

$$\sigma = \frac{Q}{A} = \frac{45879.4}{12(\pi)(8)^2} = 19.02 \text{ MPa}$$

Using grade 3 bolts (proof strength = 551 MPa), the factor of safety is:

$$\text{F.S.} = \frac{551}{19.02} = 28.9$$

2. Shear Through Verticle Leg of Angle

Bolts #7 through #11 will be in a shear mode. The centroid of this bolt group is located 80.2 mm. from point P in the x-direction.

$$\bar{x} = \frac{2(38)A+2(100)2+1(125)A}{5A}$$

$$\bar{x} = 80.2 \text{ mm.}$$

Summing forces about point P yields the force Q acting at the centroid.

$$Q = \frac{432(9309.7)}{80.2} = 50147 \text{ N}$$

Then for ten bolts,

$$d_{min} = \frac{F}{2t\tau_{ALL}} = \frac{50147}{10(2)(9.5)(37.05)} = 7.12 \text{ mm.}$$

Threads

The threads on the connecting rod and its mating connection on the upper weight pan are M16x2.

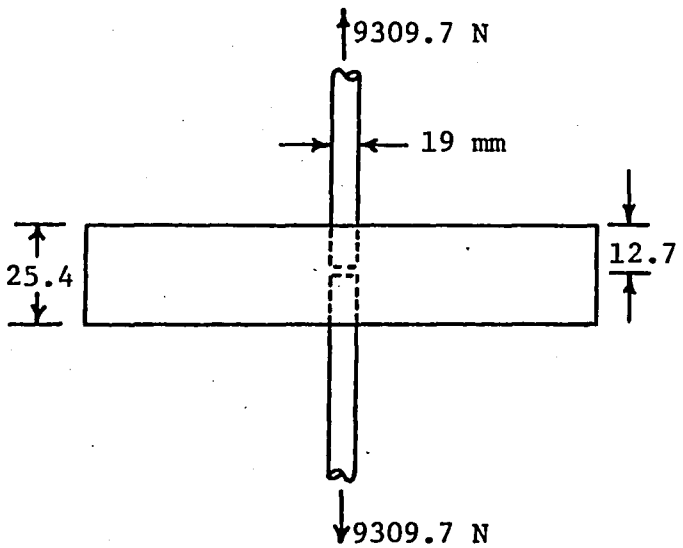

$\sigma_{ys} = 294.44$ MPa $\qquad \tau_{ALL} = 37.05$ MPa

1. Shear of Threads on Connecting Rod

$$\tau = \frac{2F}{\pi d_r h}$$

where, d_r = diameter-pitch

d_r = 19-2 = 17 mm.

Therefore,

$$\tau = \frac{2(9309.7)}{\pi(17)(12.5)} = 27.88 \text{ MPa}$$

This shear stress is less than the allowable shear stress.

2. Shear of Threads on Upper Weight Pan

$$\tau = \frac{2F}{\pi dh} = \frac{2(9309.7)}{\pi(19)(12.5)} = 24.96 \text{ MPa}$$

$$\tau < \tau_{ALL}$$

Fatigue Considerations

1. Lever Arm

A. Fatigue of ligament at A due to alternating bending stress

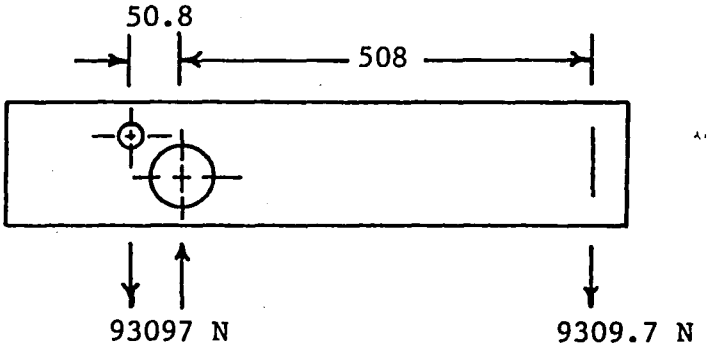

$$\sigma_{max} = \frac{(508)(9309.7)(50.8)(12)}{2(25)(102)^3} = 54.33 \text{ MPa}$$

$$\sigma_{min} = \frac{(508)(7446)(50.8)(12)}{2(25)(102)^3} = 43.46 \text{ MPa}$$

$$\sigma_{mean} = \frac{\sigma_{max} + \sigma_{min}}{2} = 48.89 \text{ MPa}$$

$$\sigma_{ALT} = \frac{\sigma_{max} - \sigma_{min}}{2} = 5.43 \text{ MPa}$$

For cold rolled steel, $S_{ult} = 448.11$ MPa. Using a surface factor of 0.82, the endurance limit becomes,

$$S_e' = (.5)(.82)(448.11) = 182.72 \text{ MPa}$$

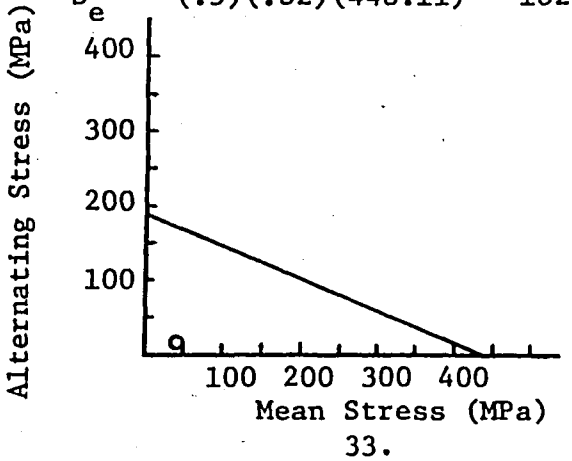

B. Shear of Bearing Shaft Through Lever Material

Using d = 60 mm.,

$$\tau_{max} = \frac{51203.35}{(2)(25)(60)} = 17.04 \text{ MPa}$$

$$\tau_{min} = \frac{40966}{(2)(25)(60)} = 13.65 \text{ MPa}$$

$$\tau_{mean} = 15.345 \text{ MPa}$$

$$\tau_{ALT} = 1.695 \text{ MPa}$$

The endurance strength is,

$$S'_{se} = (.82)(.5)(S_{su}) = 91.86 \text{ MPa}$$

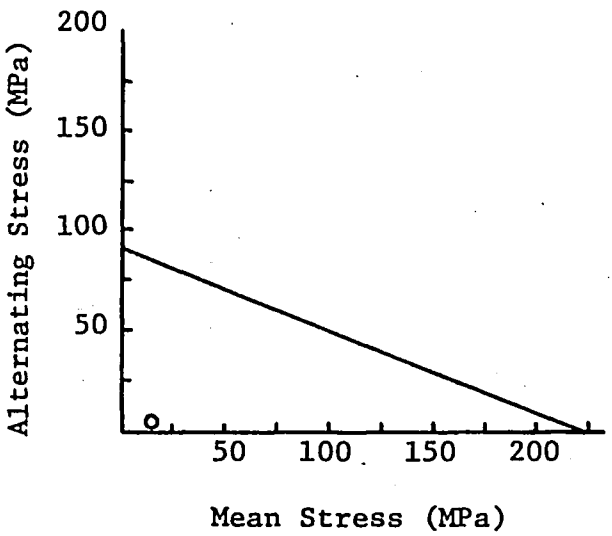

2. Grips

Taking d = 16.5 mm.,

$$\tau_{max} = \frac{46548}{2(16)(16.5)} = 88.16 \text{ MPa}$$

$$\tau_{min} = \frac{37238}{2(16)(16.5)} = 70.53 \text{ MPa}$$

$$\tau_{mean} = 79.345 \text{ MPa}$$

$$\tau_{ALT} = 8.815 \text{ MPa}$$

The endurance strength is,

$$S'_{se} = (.82)(.5)(224) = 91.86 \text{ MPa}$$

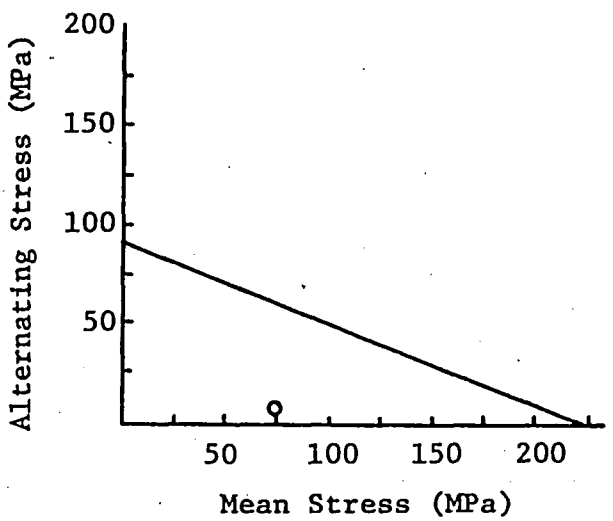

Based on these calculations it is clear that with a factor of safety of four incorporated in the sizing and selection of components, a fatigue failure as described by the Goodman diagrams above, is unlikely.

APPENDIX B

This appendix includes a table which serves as a bill of materials required to build the mechanical testing device described in this thesis. Detail and assembly drawings of the components are included in this appendix. All linear dimensions shown are in millimeters.

TABLE 1

Part or Assembly	Description of Component	Figure	
Specimen Mounting	Cold Rolled Steel, 51 mm x 150 mm x 381 mm	B4	4 Req'd
Assembly, Figure B2	Steel Angle, 76 mm x 76 mm x 150 mm x 16 mm	B3	4 Req'd
	Hot Rolled Steel, 25.4 mm x 76 mm x 152 mm	B5	4 Req'd
	Cold Rolled Steel, 38 mm x 44 mm x 92 mm	B6	2 Req'd
	Cold Rolled Steel, 38 mm x 44 mm x 145 mm	B7	2 Req'd
	108 mm O.D. Spherical Bearing, HJ-526832 Inner Race, IR-445232		4 Req'd
Grips	Cold Rolled Steel, 16 mm x 38 mm x 76 mm	B8	4 Req'd
Lever Arm	Cold Rolled Steel, 25.4 mm x 102 mm x 813 mm	B9	4 Req'd
Assembly	Spacer, Steel, 25.4 mm x 38 mm x 90 mm	B10	6 Req'd
Weight Hanger	Hot Rolled Steel	B11	2 Req'd
Bracket			
Frame (Figure B26)	Steel Tube, 6.35 mm Thick:		
	76 mm x 76 mm x 2134 mm		2 Req'd
	76 mm x 76 mm x 1981 mm		1 Req'd
	76 mm x 76 mm x 230 mm		2 Req'd
	76 mm x 76 mm x 1219 mm		1 Req'd

TABLE 1 (Continued)

Part or Assembly	Description of Component	Figure	
	Steel Angle, 76 mm x 76 mm x 571 mm x 3.175 mm		2 Req'd
	Steel Angle, 76 mm x 76 mm x 86 mm x 9.5 mm		2 Req'd
Loading Assembly	12.7 mm Bore Linear Bearing: TWN-8		2 Req'd
	12.7 mm Dia. Ground Shaft: 12.7 mm x 203 mm		2 Req'd
	9.5 mm Bore Linear Bearing: Super 6		8 Req'd
	9.5 mm Dia. Ground Shaft: 9.5 mm x 76 mm		8 Req'd
	25.4 mm Bore Pillow Block - Rak Fafnir		4 Req'd
	Cam - 51 mm Dia. Rd. Shaft, 4.75 mm - Offset Bore	B16	2 Req'd
	Linear Bearing Bracket, 6 mm Steel	B17	2 Req'd
	Cam Follower, YCR-32		2 Req'd
	Fixture, Cam Follower	B18	2 Req'd
Spring Plate	Hot Rolled Steel, 25.4 mm x 203 mm x 203 mm	B12	2 Req'd
	Fastener, Steel	B13	2 Req'd
Lower Weight Pan	Hot Rolled Steel, 19 mm x 203 mm x 203 mm	B14	2 Req'd
Upper Weight Pan	Hot Rolled Steel, 25.4 mm x 203 mm x 203 mm	B15	2 Req'd
Upper Connecting Rod	20 mm Dia. Rd. Steel Rod	B24	2 Req'd

TABLE 1 (Continued)

Part or Assembly	Description of Component	Figure	
Lower Connecting Rod	20 mm Dia. Rd. Steel Rod	B23	2 Req'd
Wide Flange	Steel, 152 mm x 1372 mm	B20	1 Req'd
Wide Flange	Steel, 152 mm x 711 mm	B22	1 Req'd
I-Beam	Steel, 152 mm x 1676 mm	B19	1 Req'd
Angle	Steel, 76 mm x 76 mm x 533 mm x 6 mm		2 Req'd
Motor Mt. Brk't	6 mm Steel	B25	2 Req'd
Gusset	6 mm Steel	B21	16 Req'd
Angle	Steel, 76 mm x 76 mm x 1270 mm x 6 mm		2 Req'd

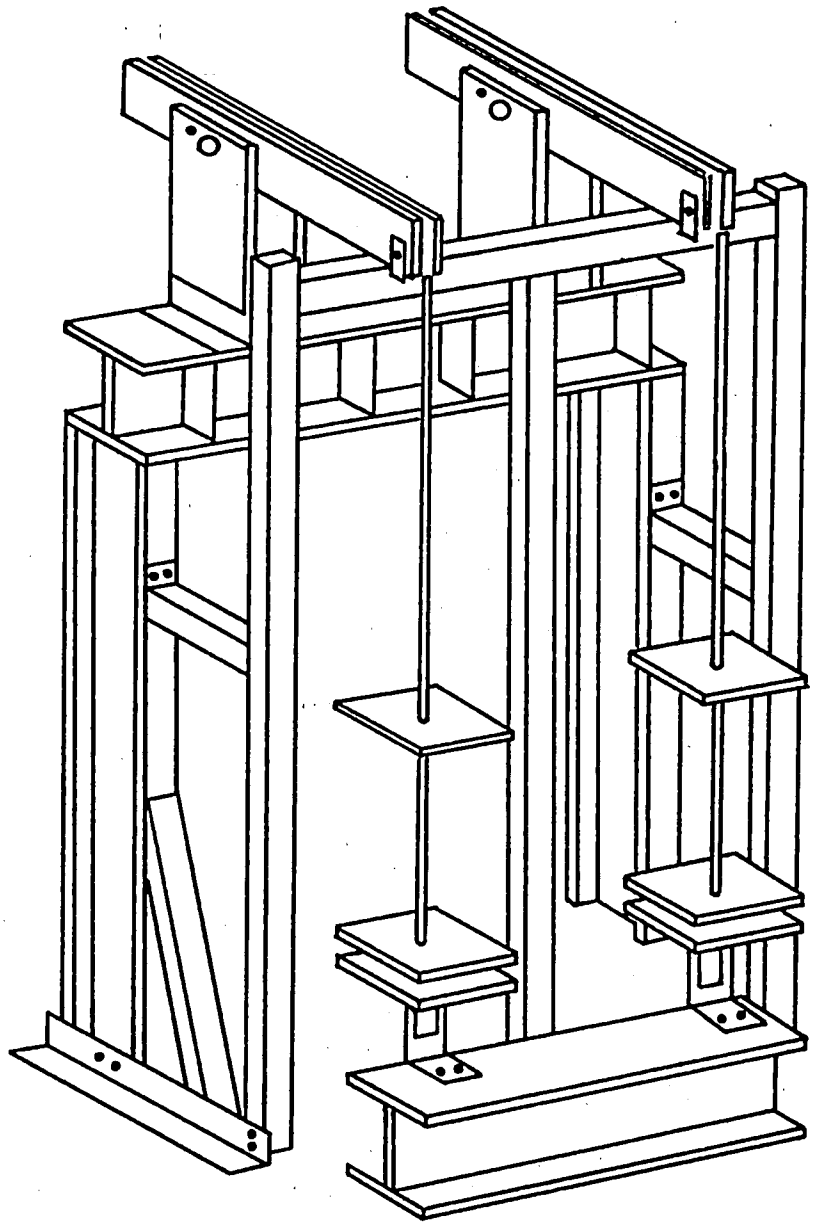

Figure B1.

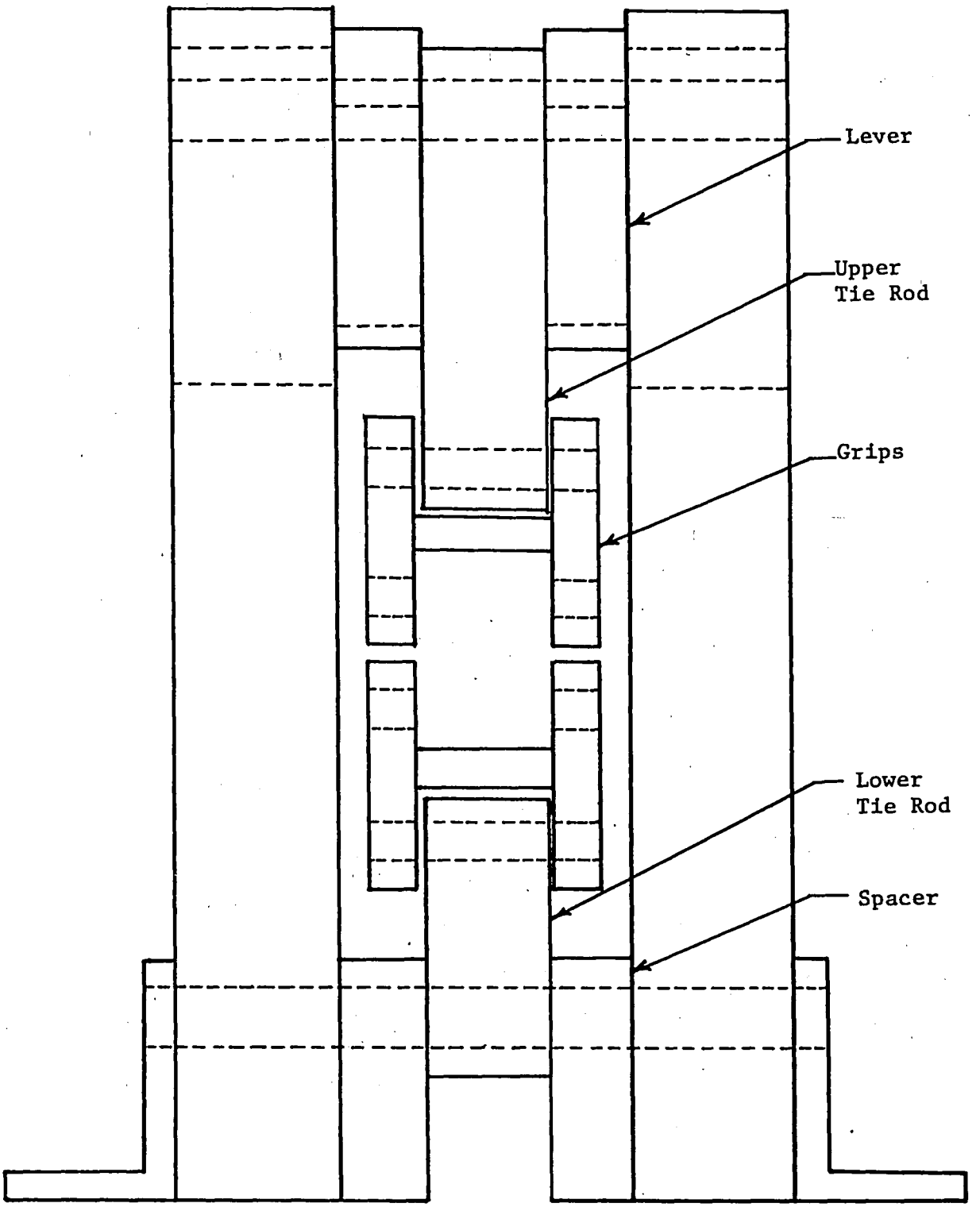

Figure B2. Specimen Mount Assembly

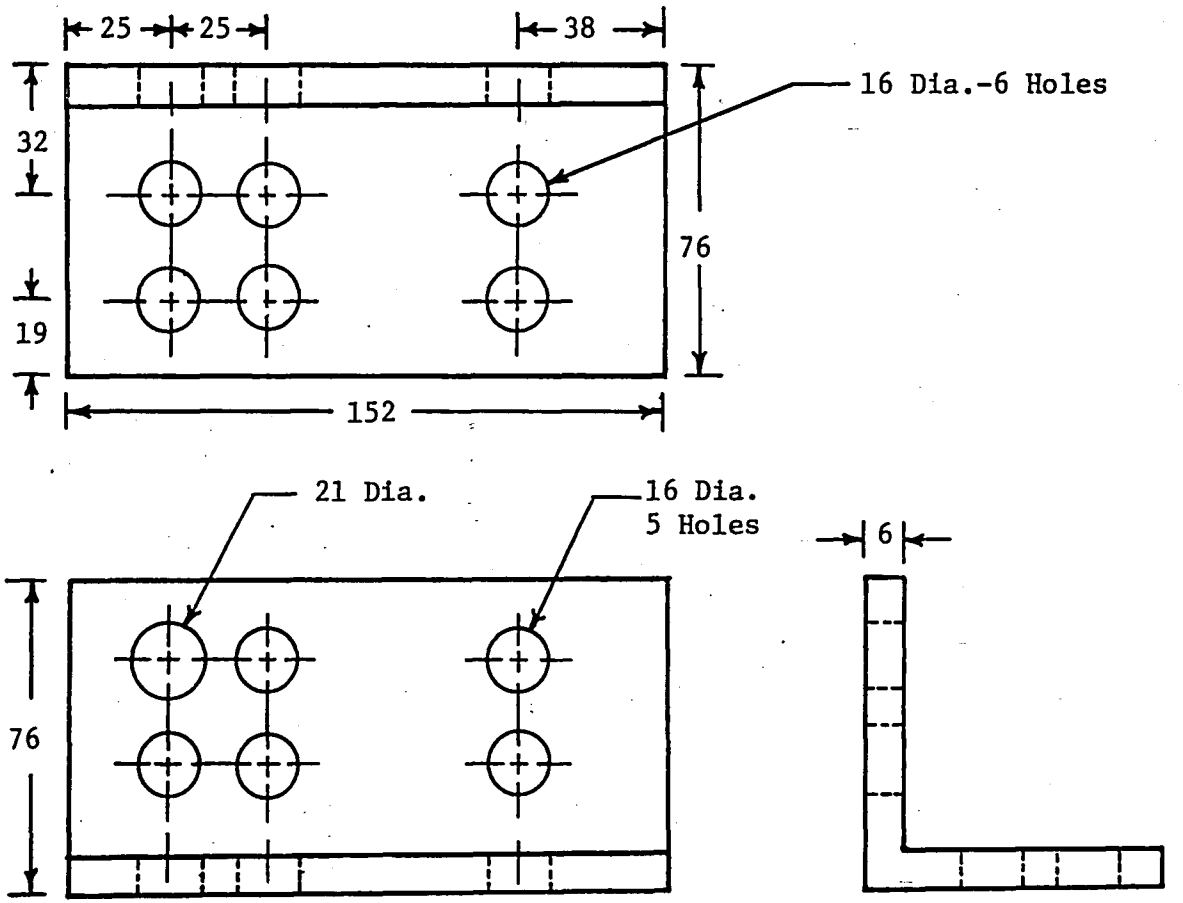

Figure B3. Angle, Specimen Mounting Assembly

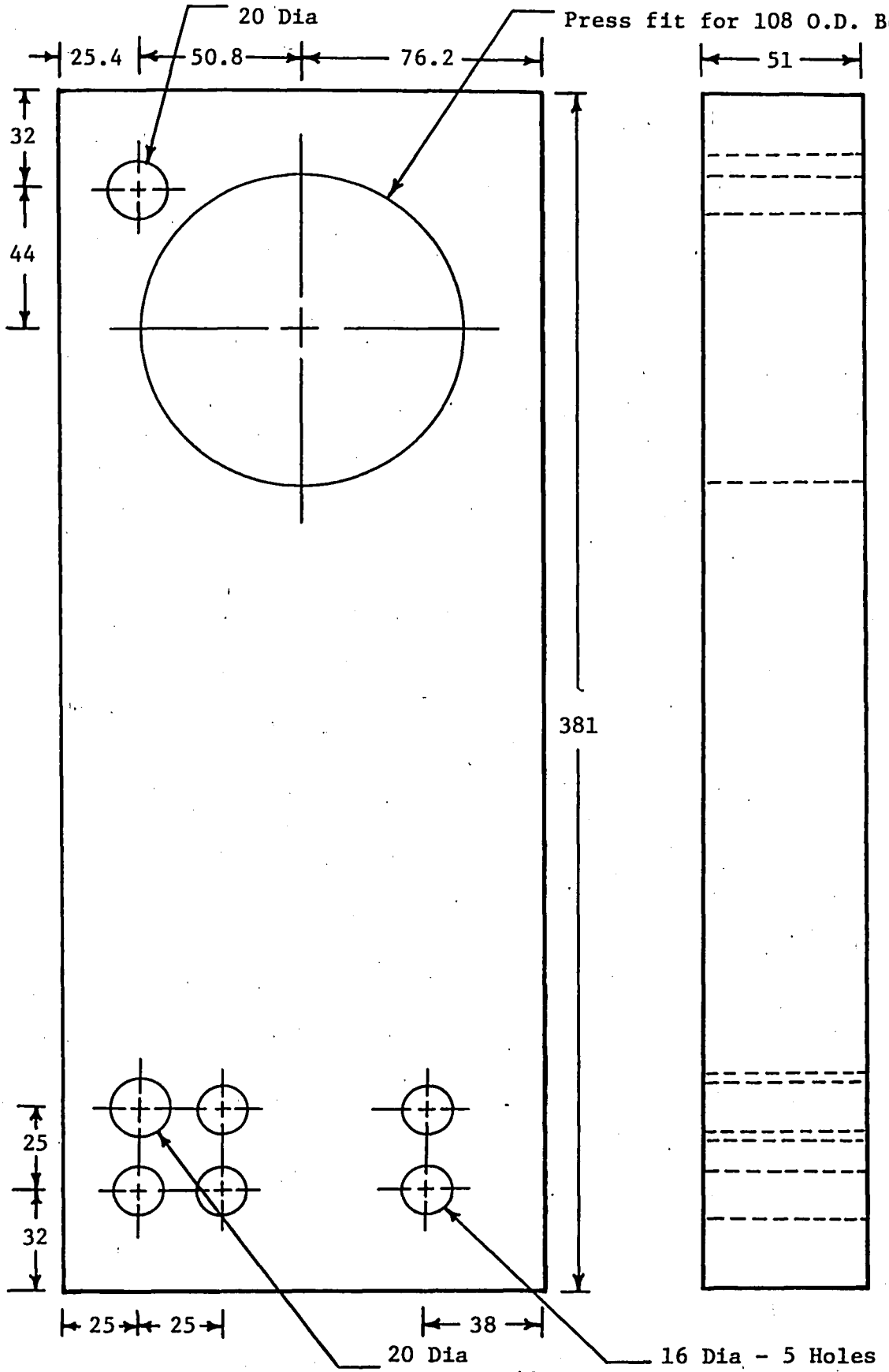

Figure B4. Plate, Specimen Mounting Assembly

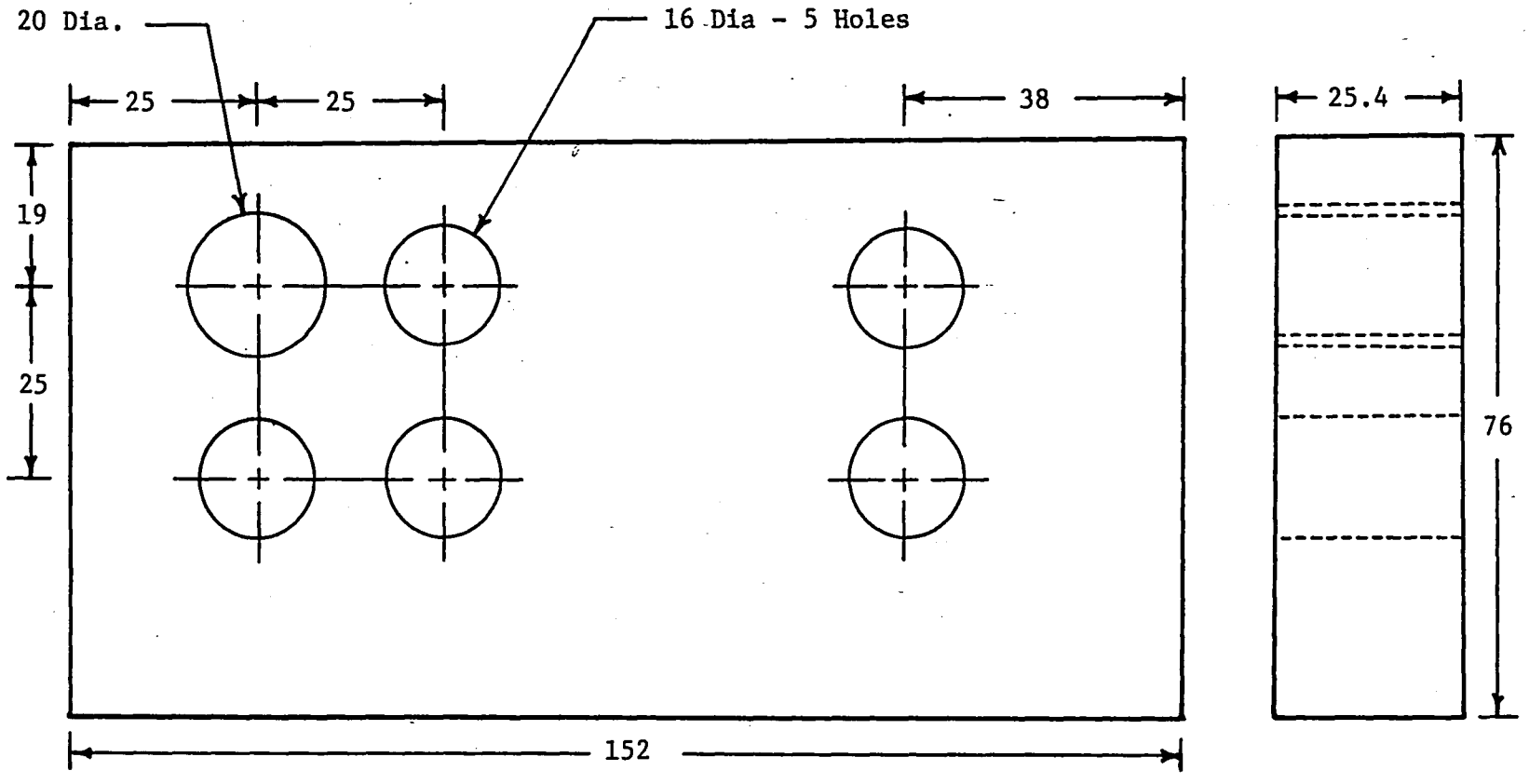

Figure B5. Spacer, Specimen Mounting Assembly

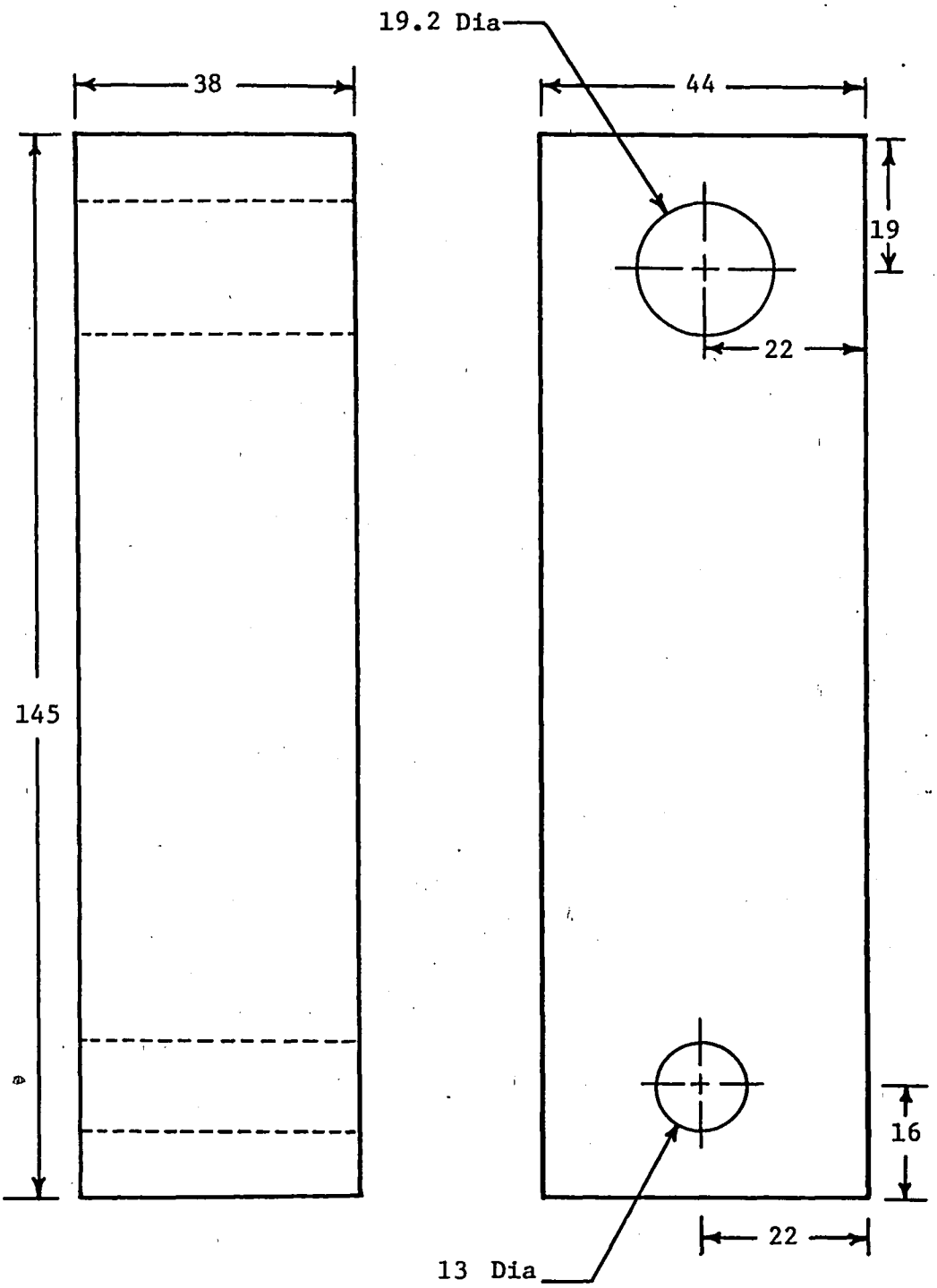

Figure B6. Upper Tie Rod, Specimen Mounting Assembly

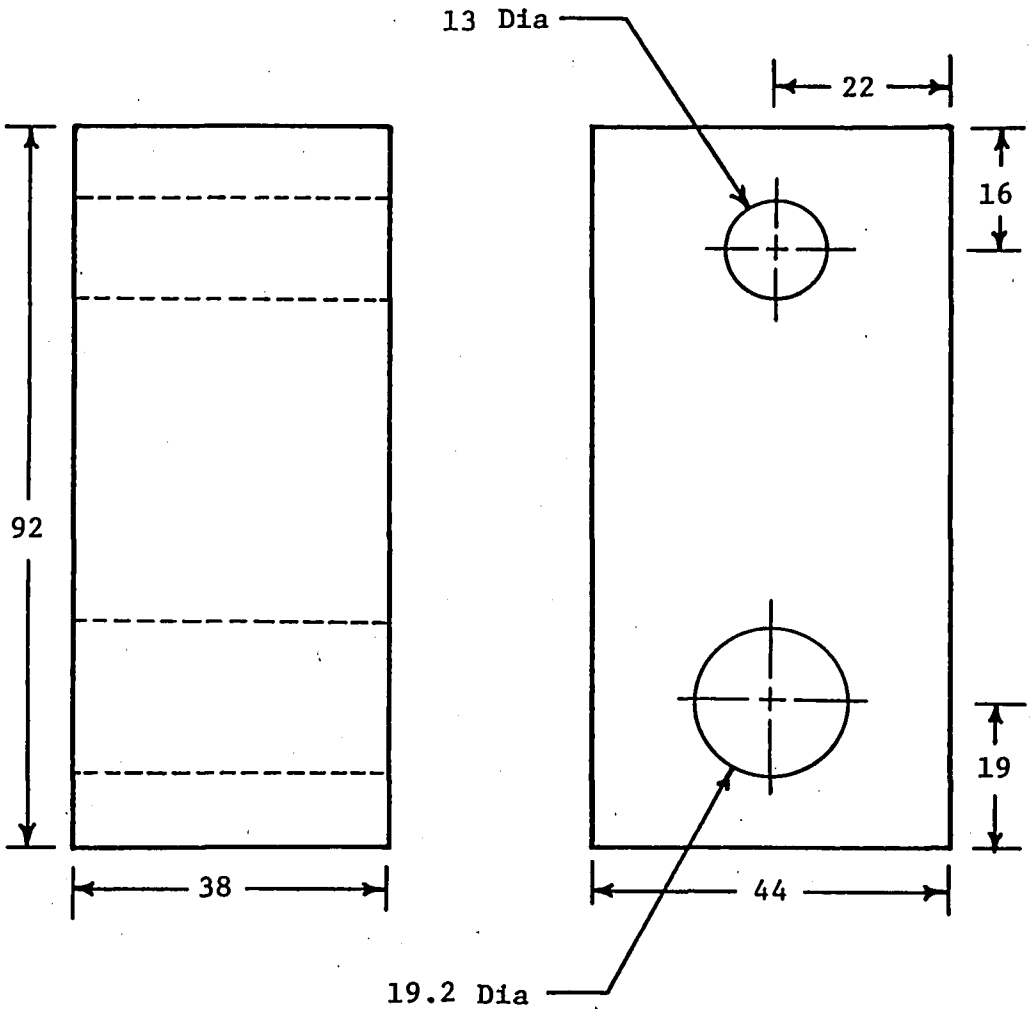

Figure B7. Lower Tie Rod, Specimen Mounting Assembly

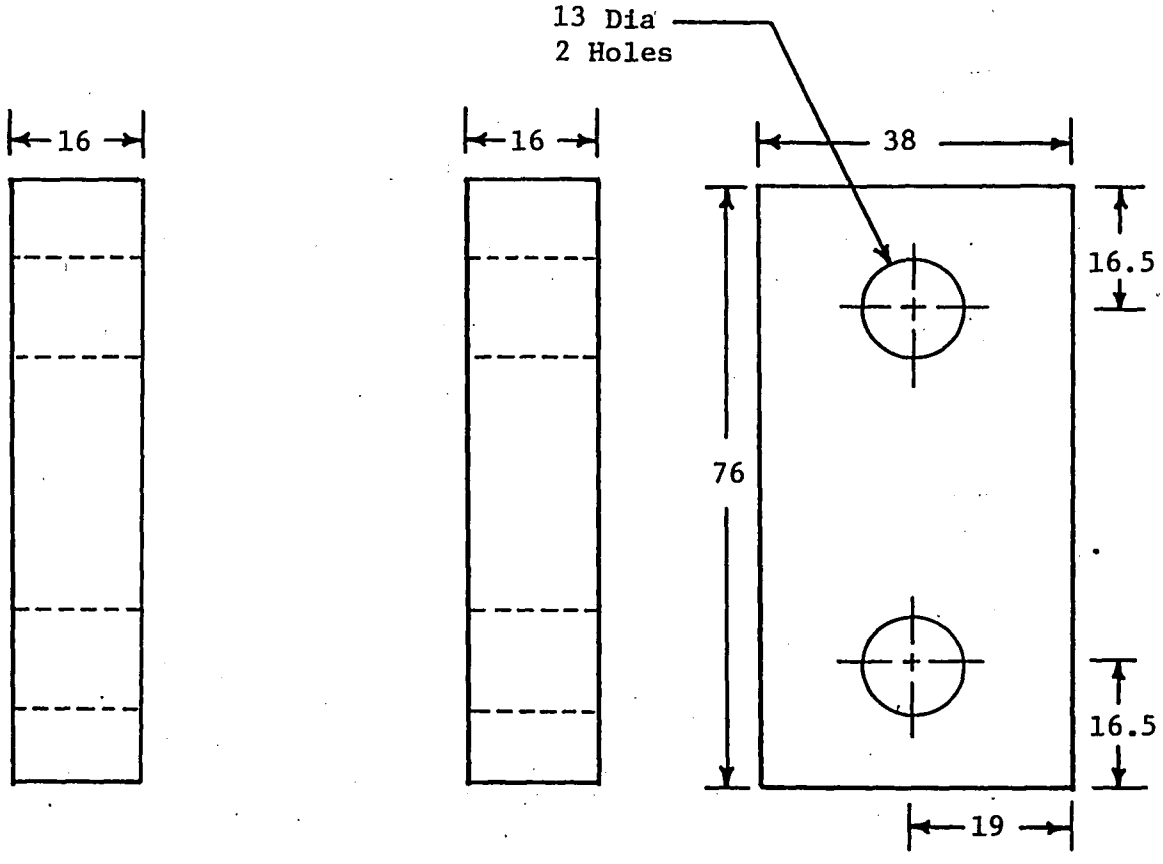

Figure B8. Grip

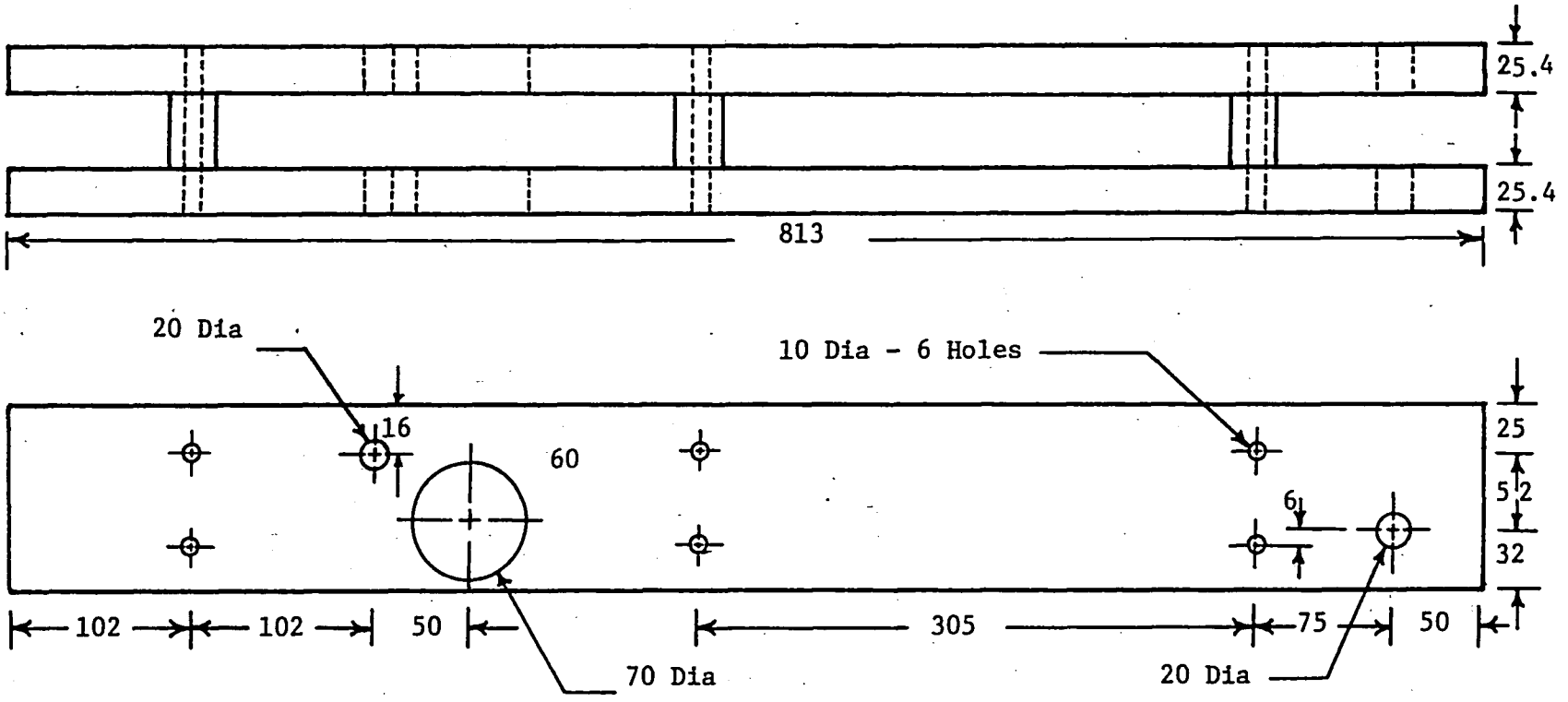

Figure B9. Lever Arm Assembly

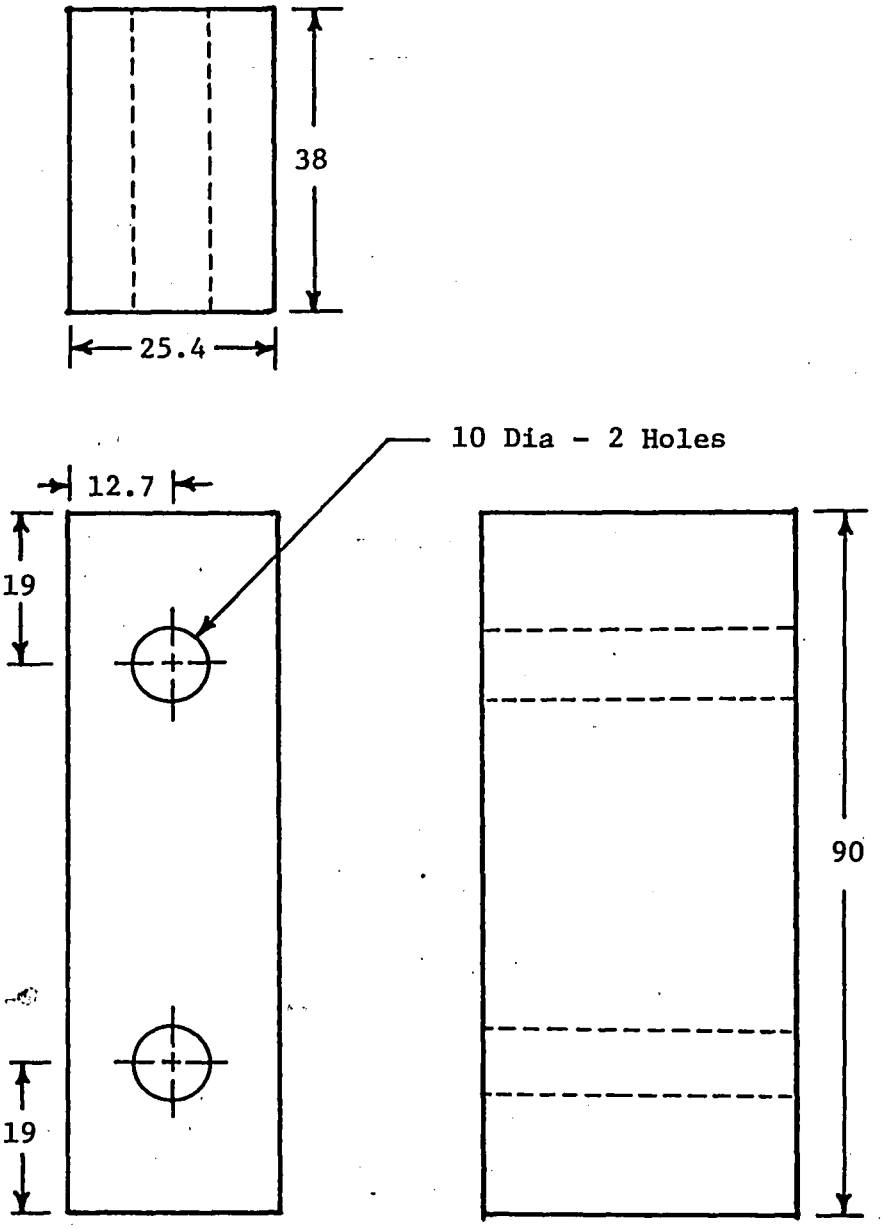

Figure B10. Spacer, Lever Arm

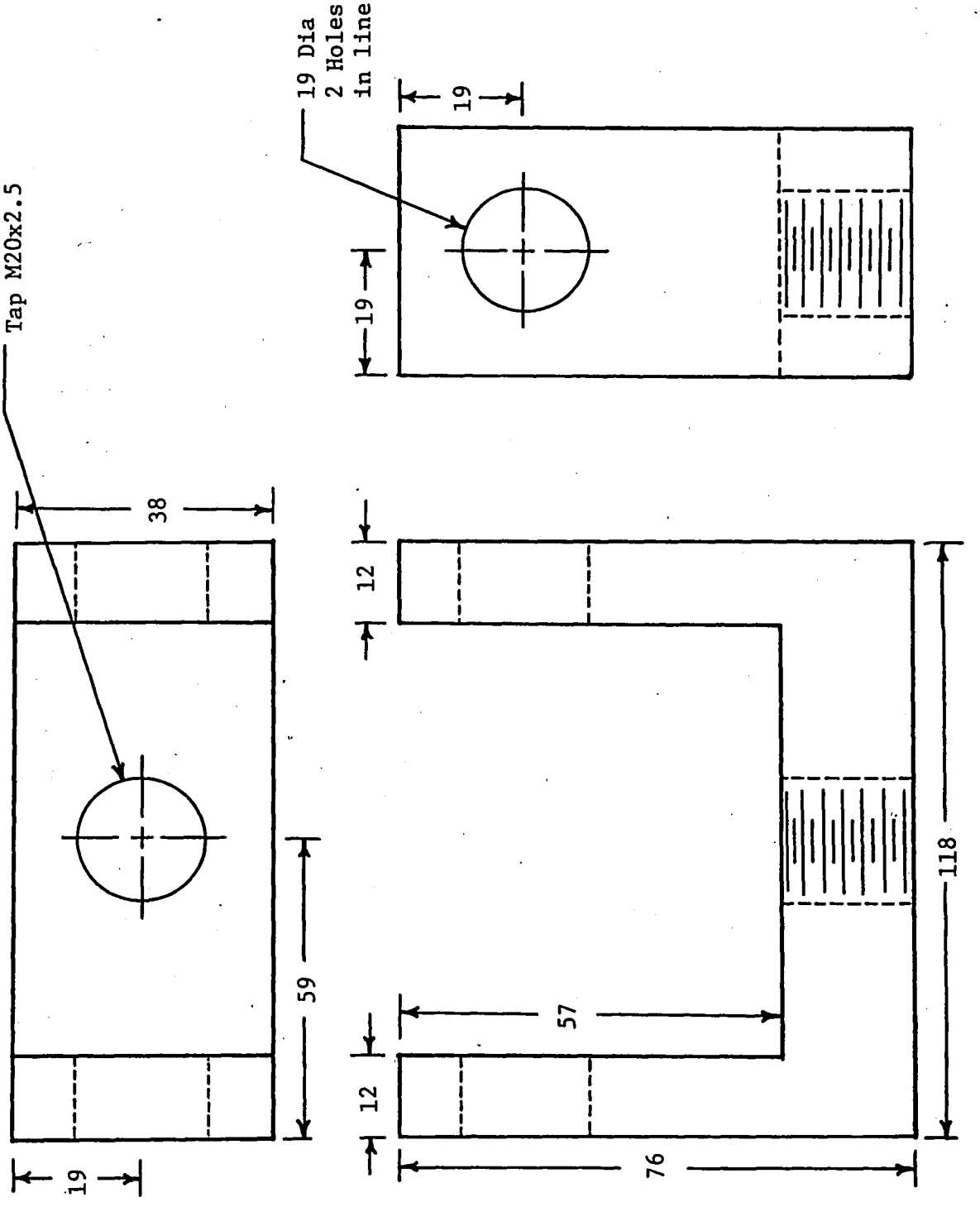

Figure B11. Weight Hanger Bracket

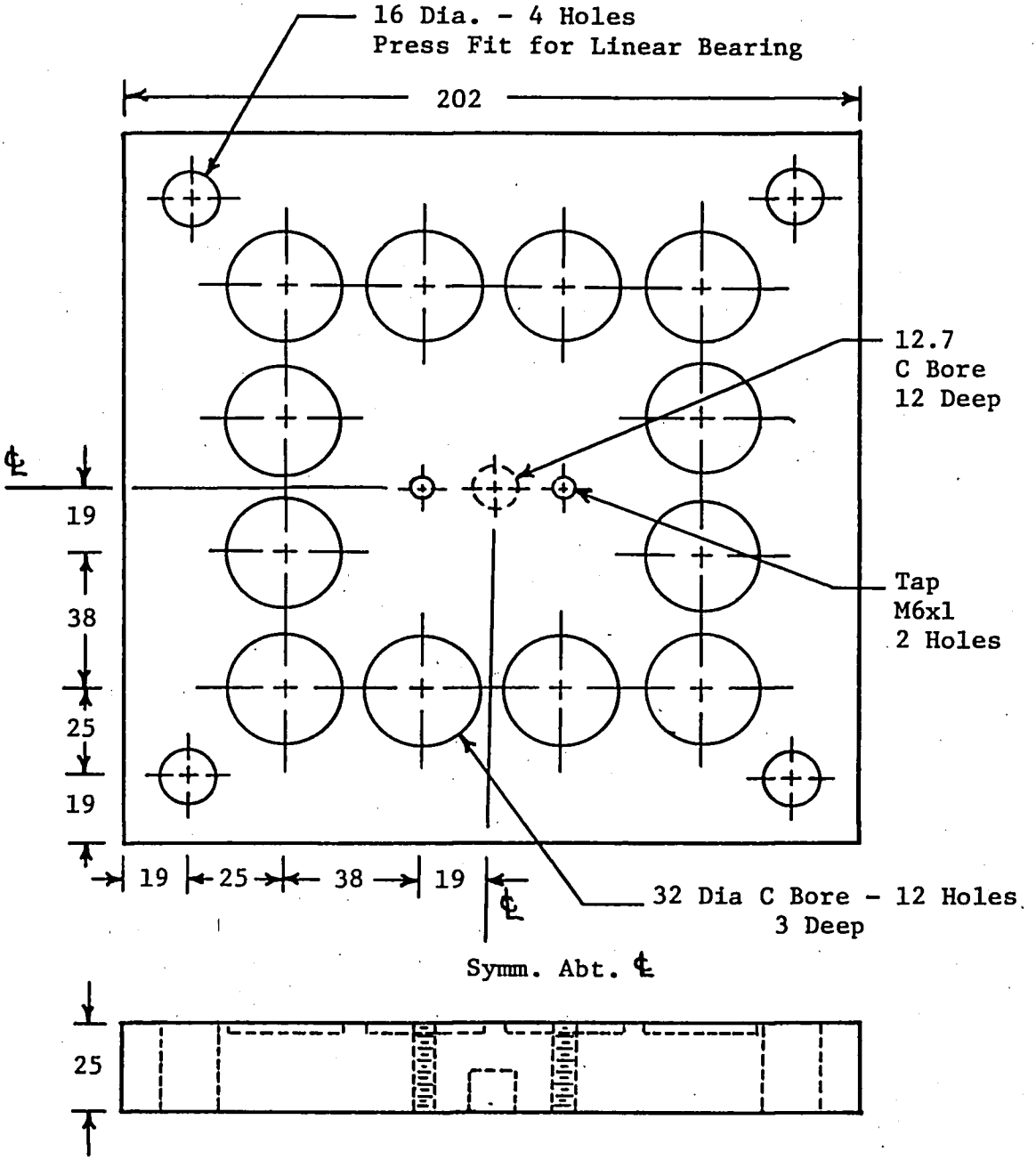

Figure B12. Spring Plate

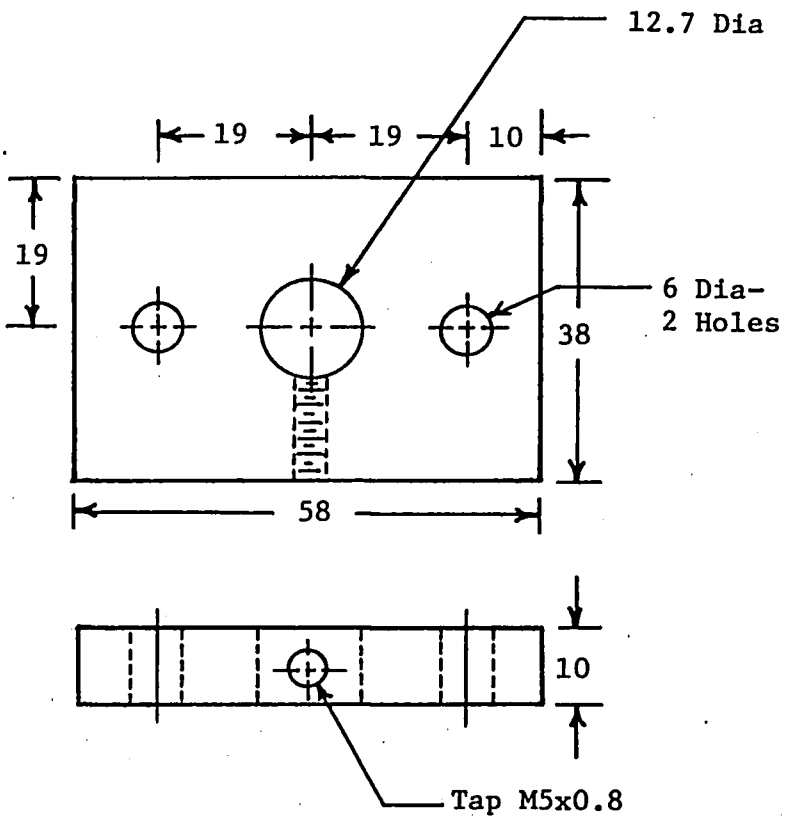

Figure B13. Fastener, Spring Plate

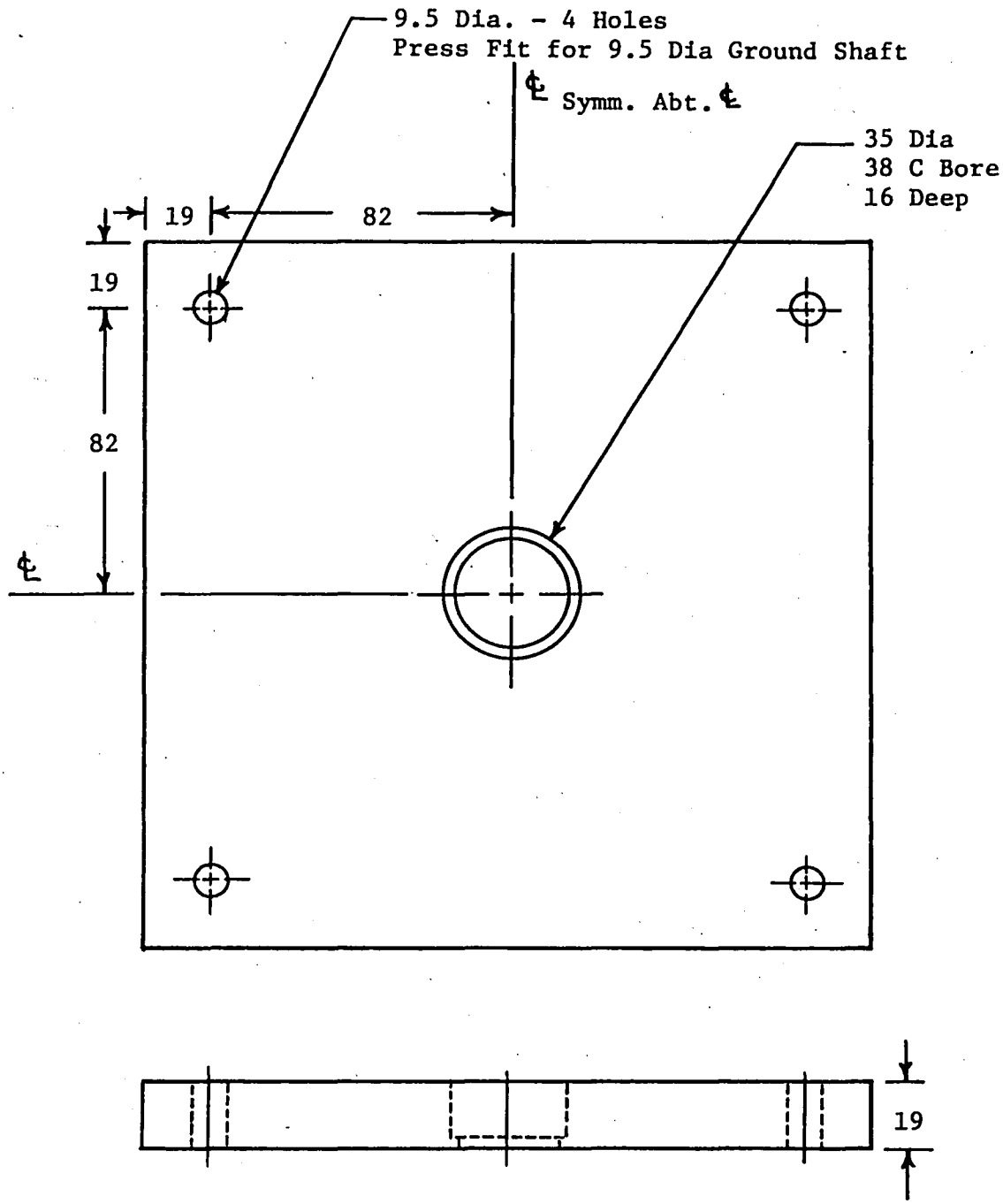

Figure B14. Lower Weight Pan

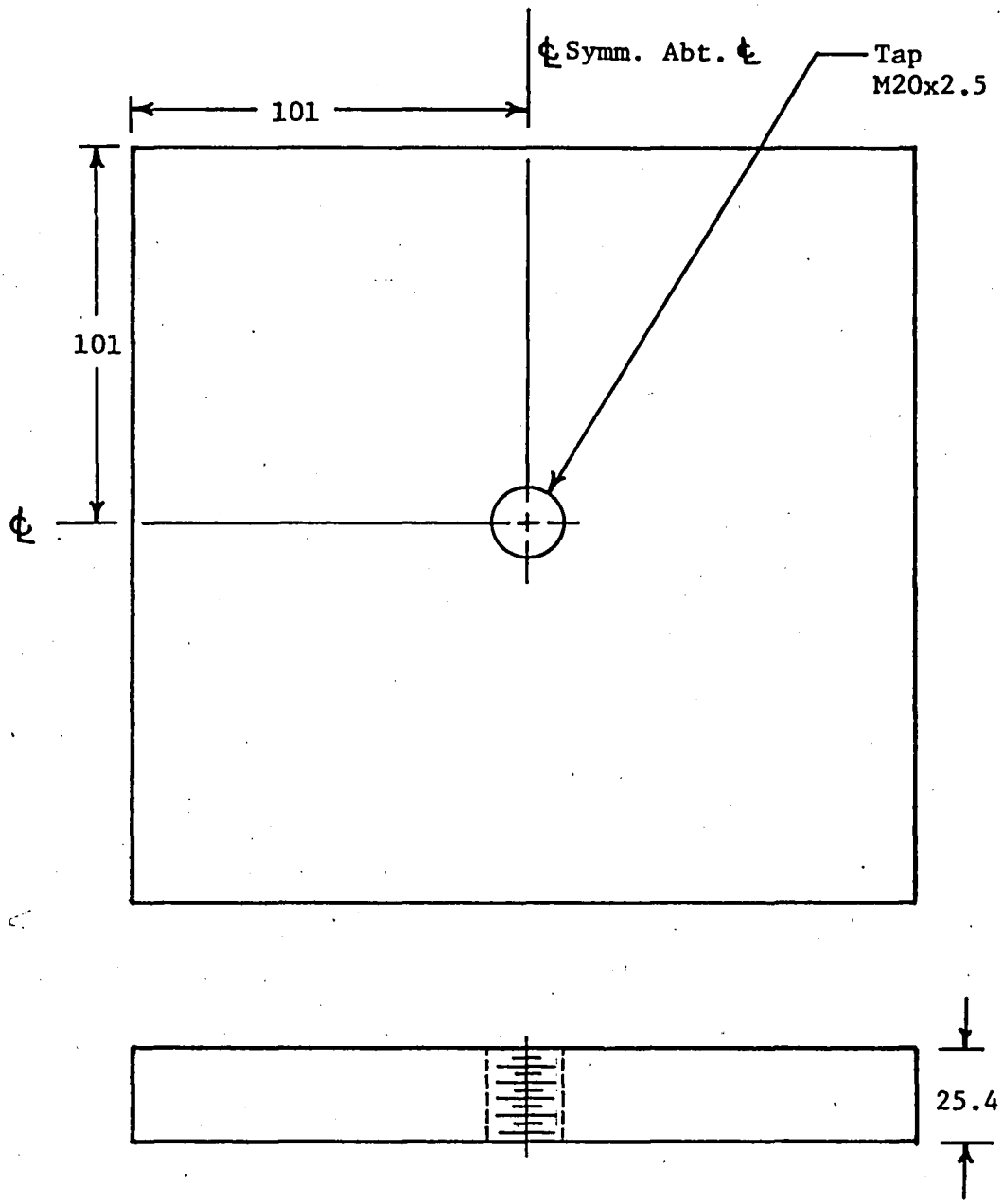

Figure B15. Upper Weight Pan

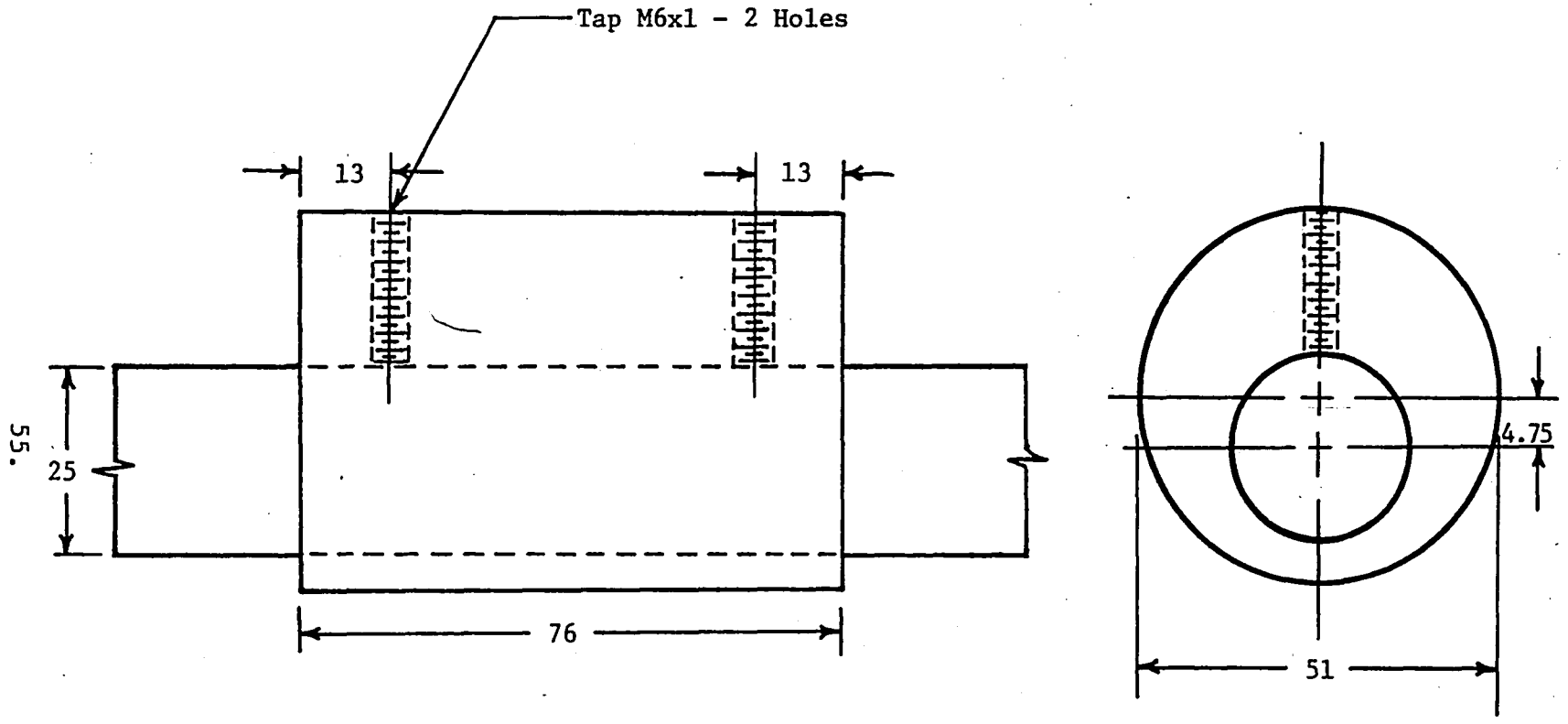

Figure B16. Cam Shaft

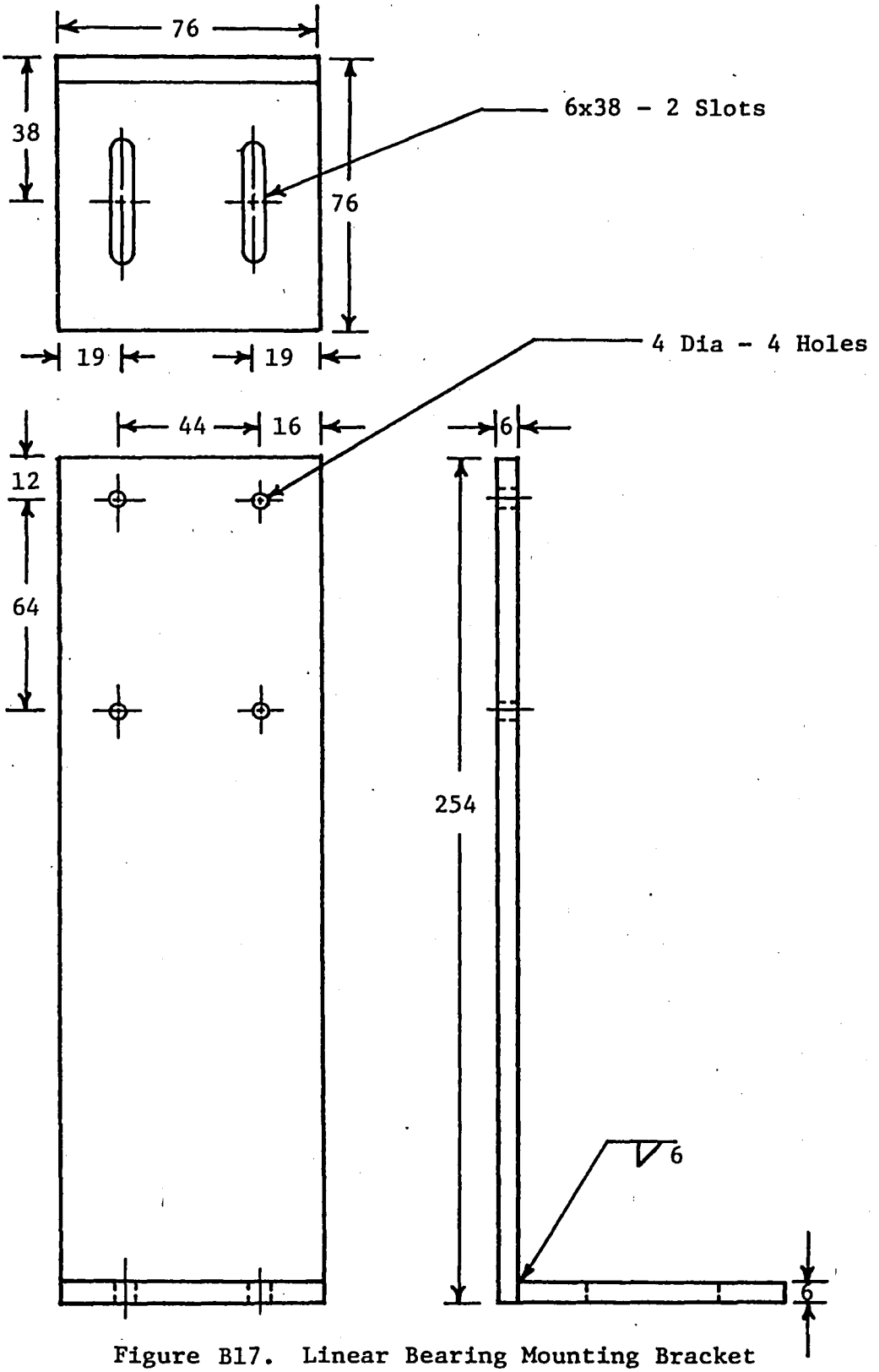

Figure B17. Linear Bearing Mounting Bracket

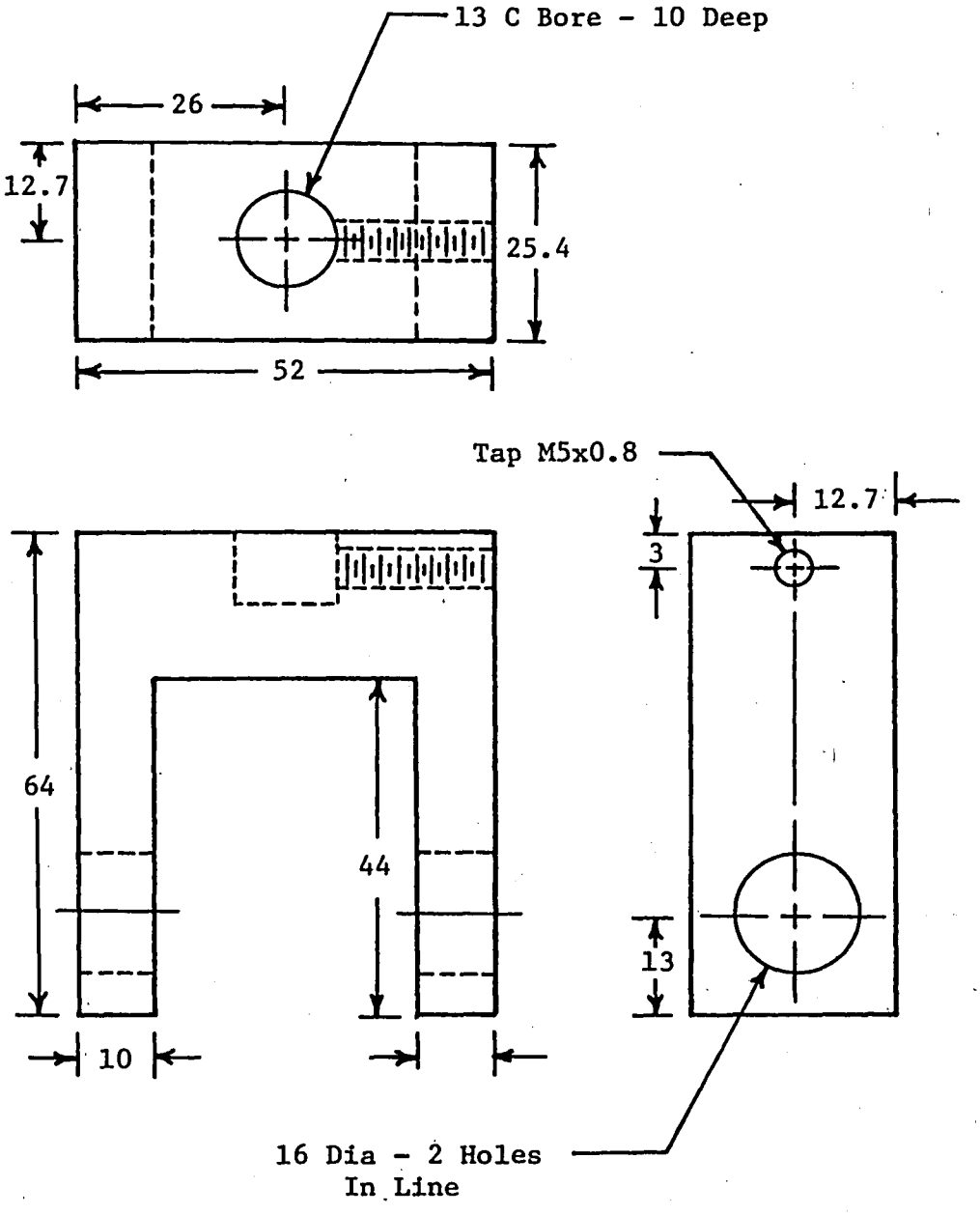

Figure B18. Fixture, Cam Follower

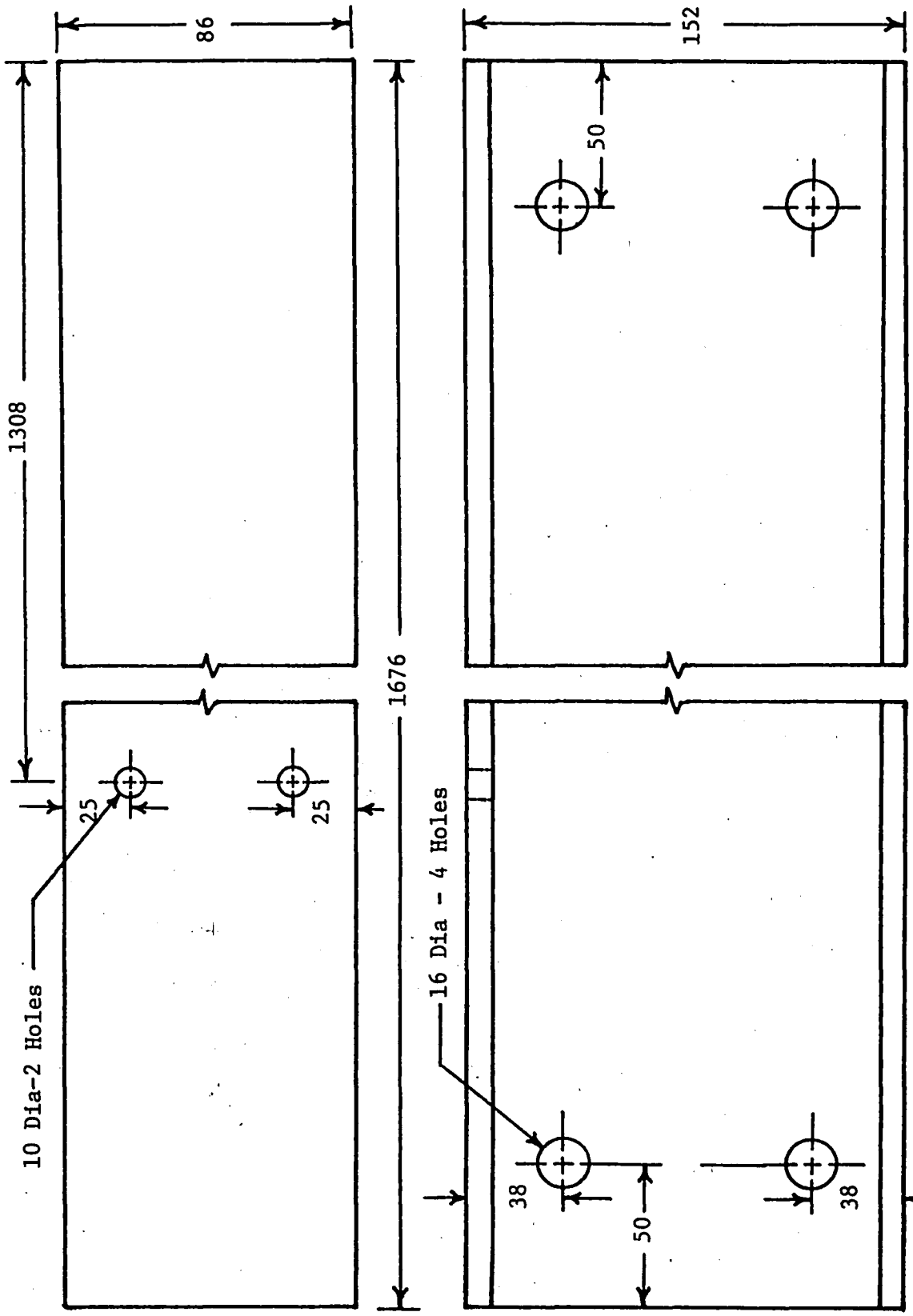

Figure B19. I-Beam

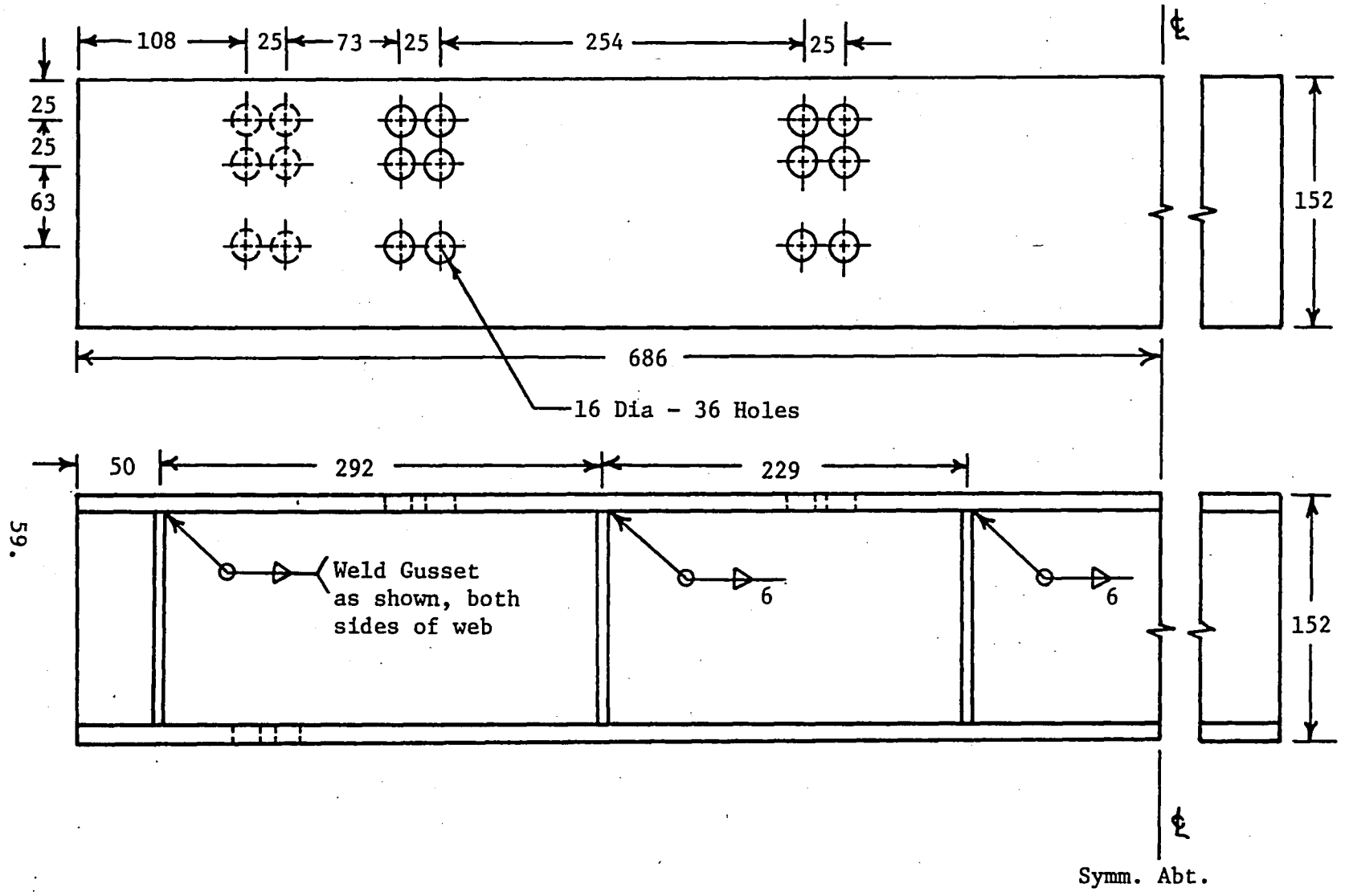

Figure B20. Upper Wide Flange

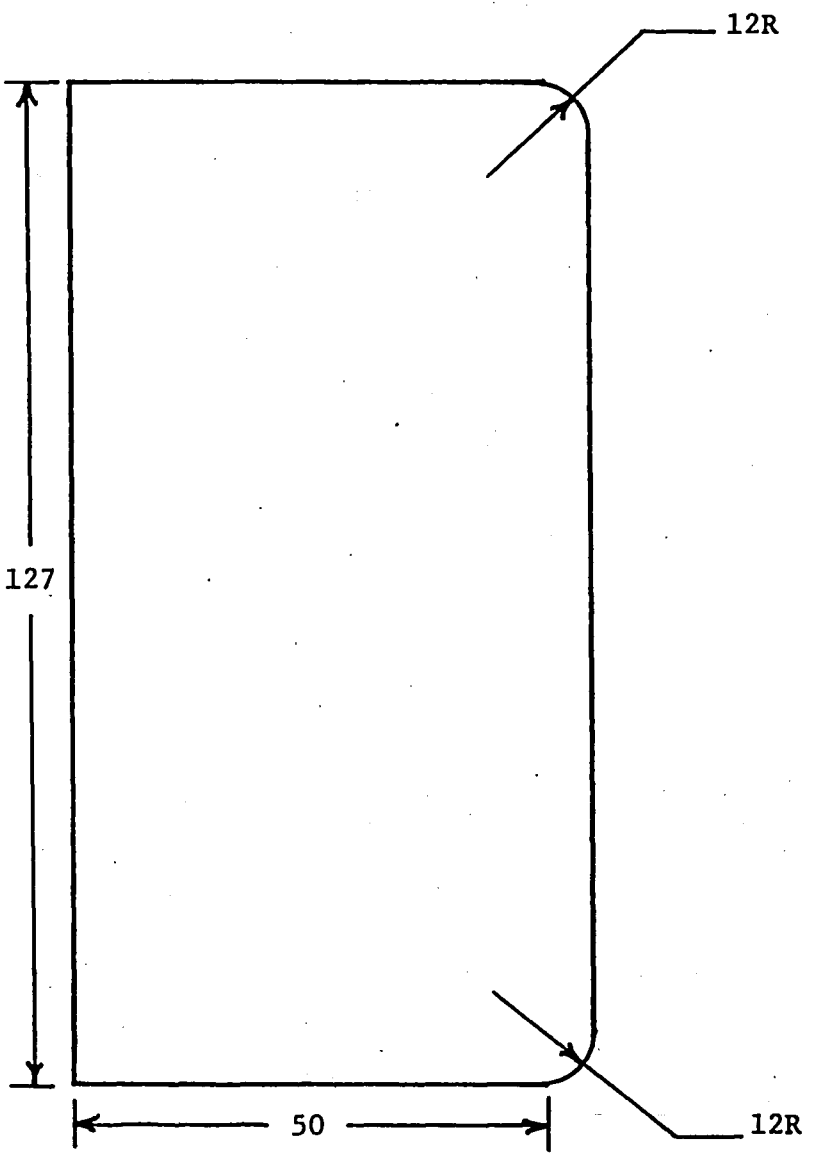

Figure B21. Gusset

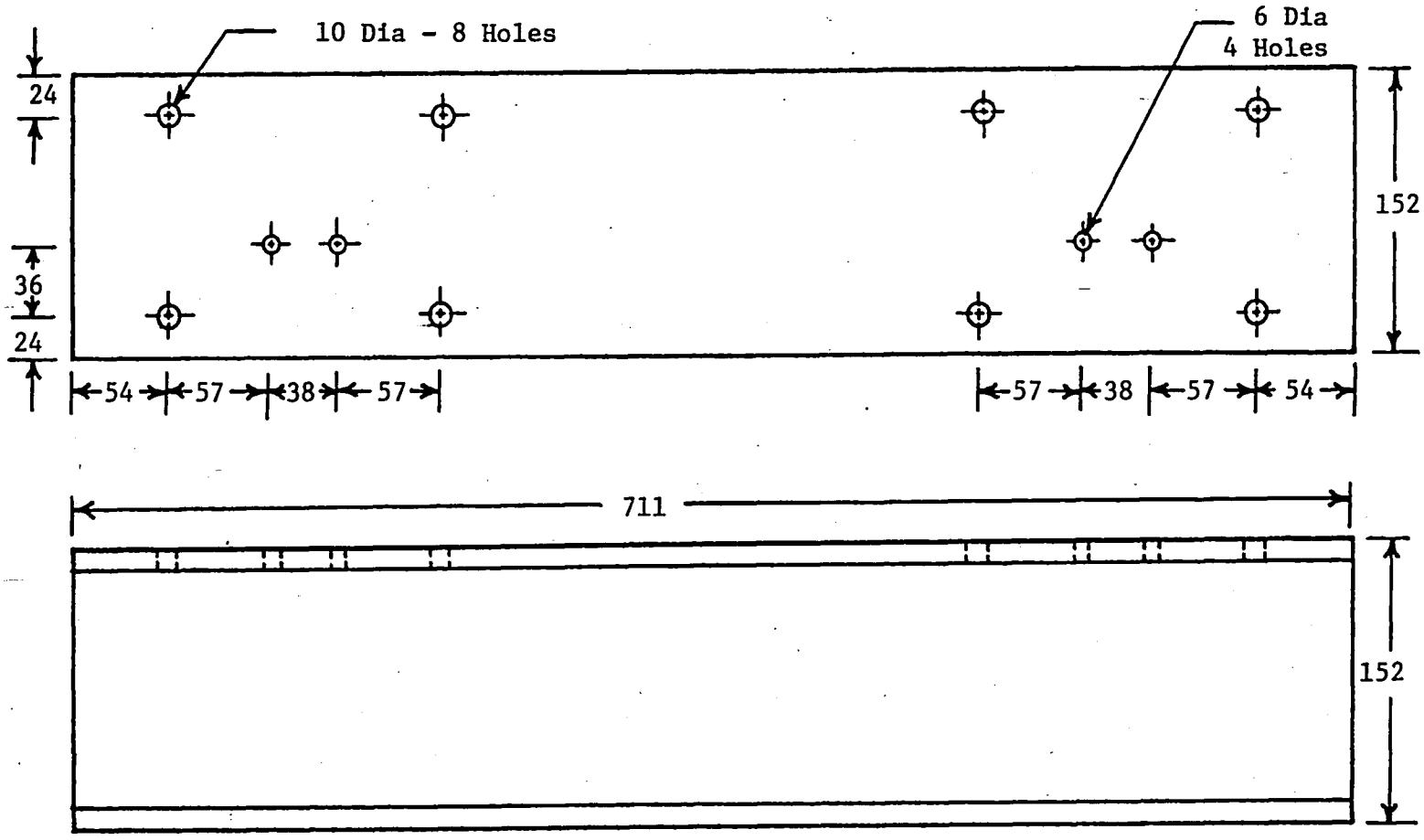

Figure B22. Lower Wide Flange

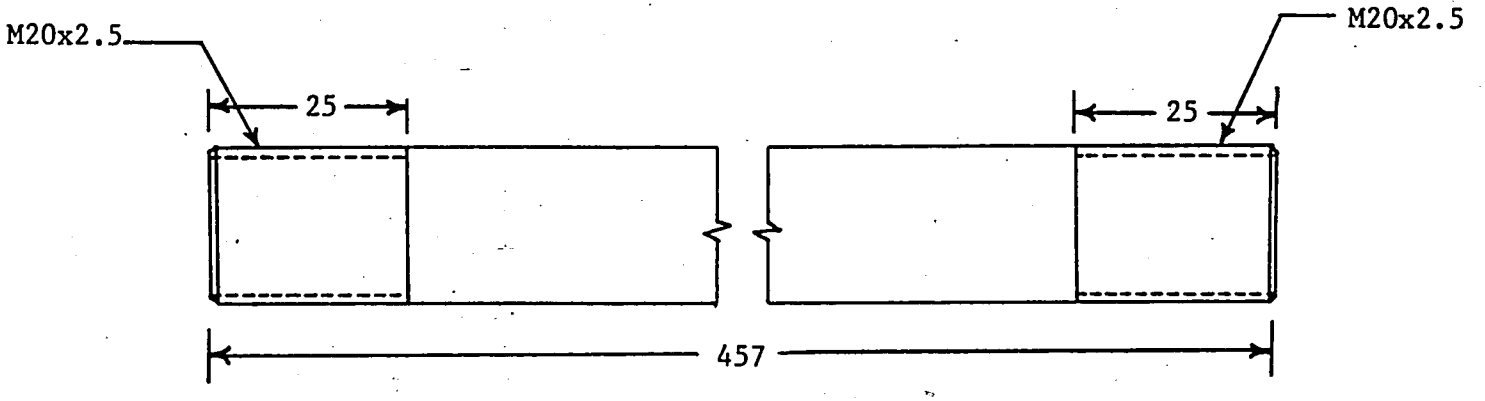

Figure B23. Lower Connecting Rod

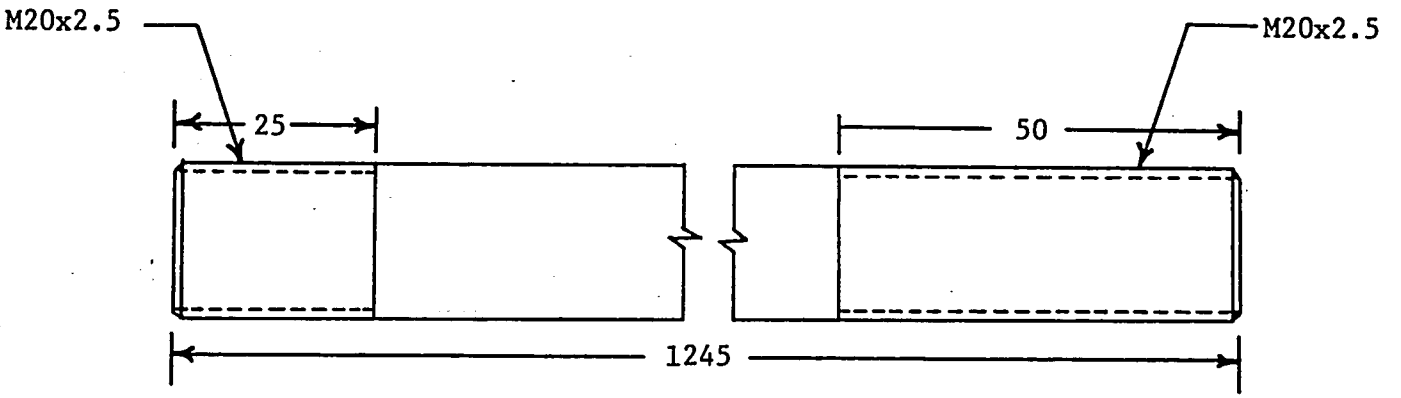

Figure B24. Upper Connecting Rod

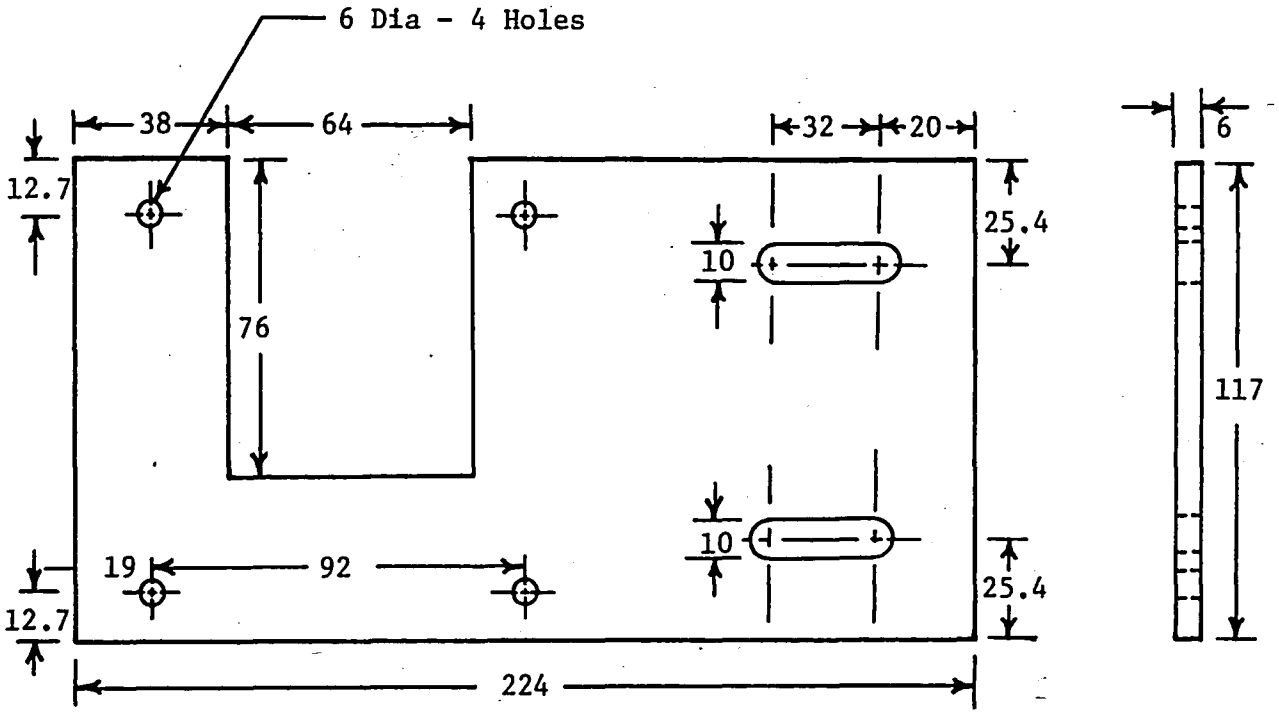

Figure B25. Motor Mounting Bracket

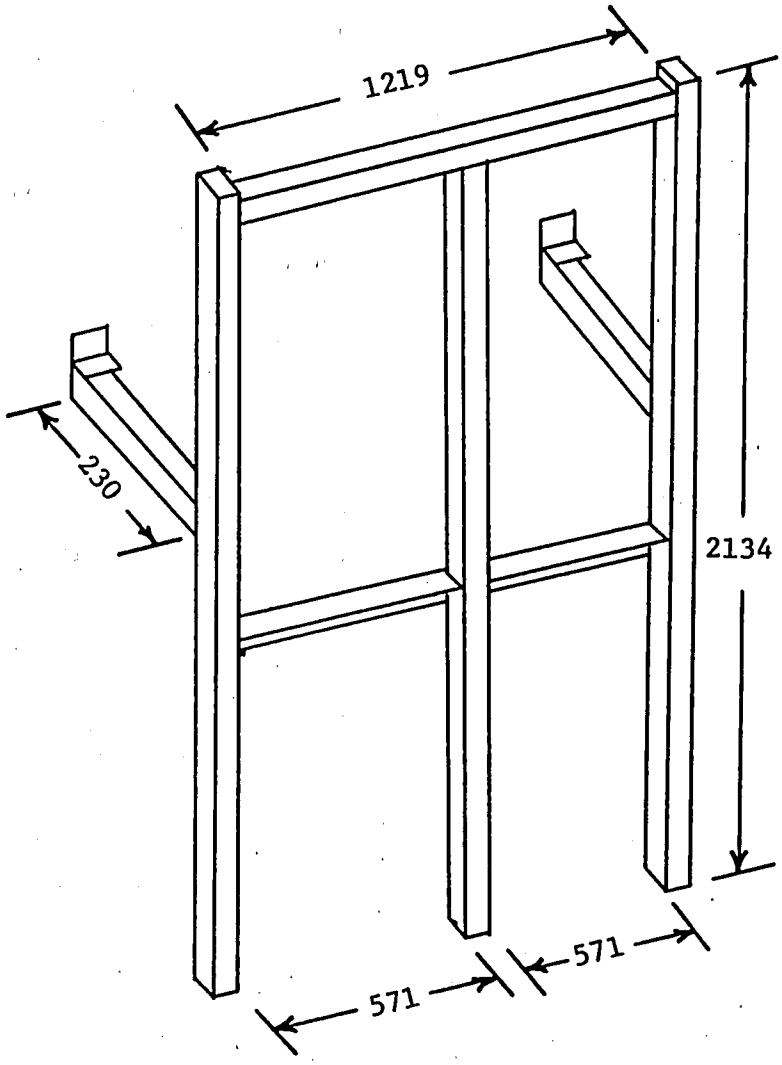

Figure B26. Frame

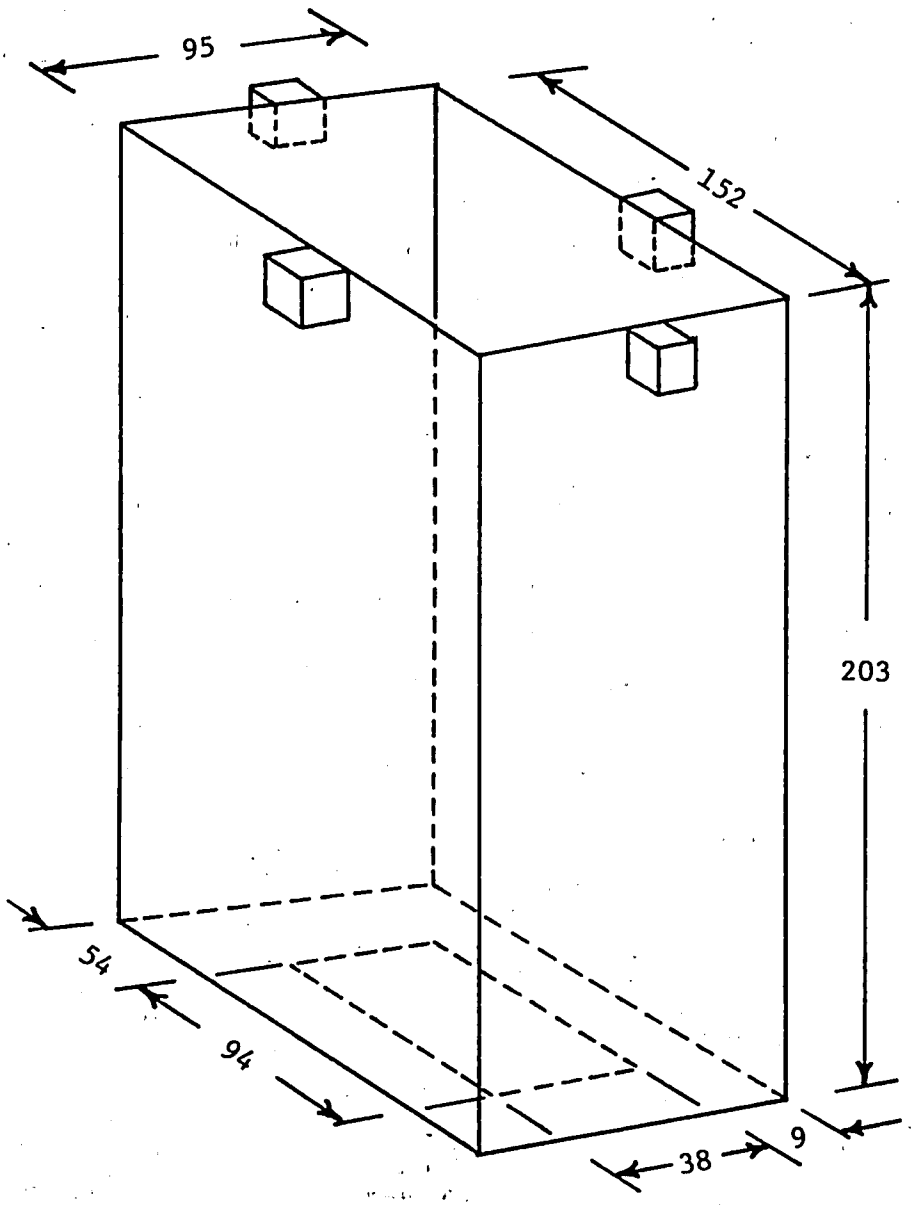

Figure B27. Environmental Chamber

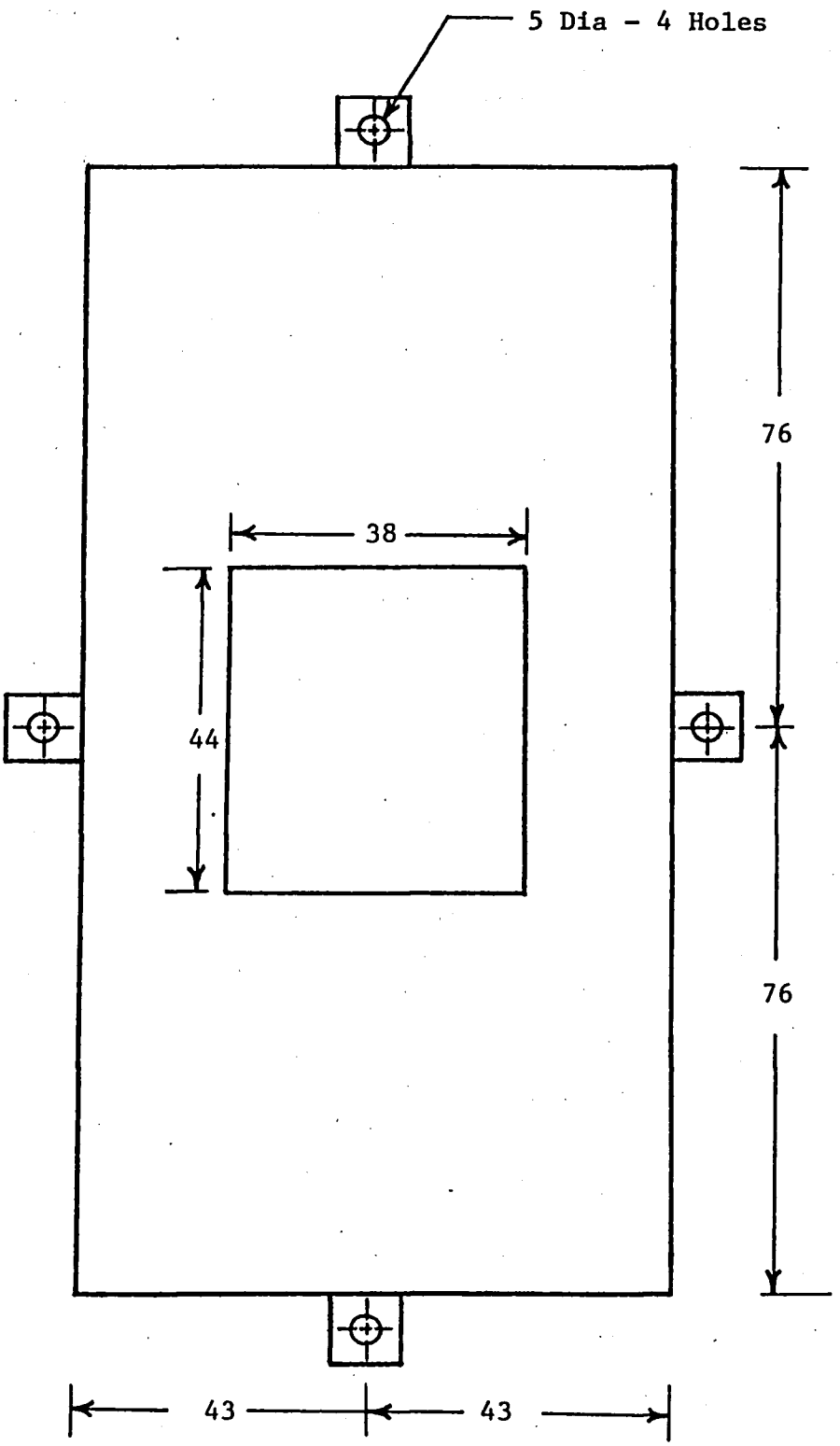

Figure B28. Cap, Environmental Chamber

BIOGRAPHY

Timothy P. Brinker was born in Allentown, Pennsylvania on May 1, 1955 to Gail and Donald P. Brinker. He attended Moravian College in Bethlehem, Pennsylvania from 1973 to 1977 where he received a B.S. in Mathematics. After being enrolled in the Graduate School at Lehigh University from 1977 to 1979 he took an engineering position with Mack Trucks within the Vehicle Development and Test Center in Allentown. Then, working during the evenings a thesis to be presented to the Graduate Committee in candidacy for the degree of Master of Science in the Department of Mechanical Engineering was completed in January 1980.